Effects Of Marine Micro And Macroalgae Building Blocks On Strength Development In Green Cement Composites

Li-Yuan Lin (Josh Lin)

A thesis
submitted in partial fulfillment of the
requirements for the degree of
Master of Science

University of Washington
2023
Committee:
Eleftheria Roumeli
Dwayne D. Arola

Program Authorized to Offer Degree*:*
Department of Materials Science and Engineering

University of Washington

ABSTRACT

Effects Of Marine Micro And Macroalgae Building Blocks On Strength Development In Green Cement Composites

Li-Yuan Lin

Chair of the Supervisory Committee:

Eleftheria Roumeli

Department of Materials Science and Engineering

The utilization of biomass-based green cement has gained significant attention in the concrete industry as sustainability becomes a key focus. Among the available biobased additions, marine algal materials have emerged as a promising candidate due to their advantageous features such as rapid growth rate and efficient carbon sequestration. However, incorporating algae into the cement matrix presents challenges, involving hindrance and retardation of the hydration reactions, leading to a decline in the mechanical properties of algae green cement. In this study, we aimed to investigate the chemical interactions between two types of algae fillers, namely spirulina and ulva, and the cement matrix. Initially, we examined the interaction in a simplified

chemical system using biopolymer representatives (glucomannan, lactalbumin, sucrose, and stearic acid). The results demonstrated a significant decrease in the mechanical properties of glucomannan and alpha-lactalbumin cement composites. Consequently, we conducted a study involving extraction-modified algae-cement composites to investigate further the interaction between the algae fillers and the cement matrix. We found that both hot and cold water-extracted spirulina and ulva resulted in an improvement in compressive strength. Furthermore, the formation of distinct nanofibers in 500-700 nm within the matrix was observed in the case of lactalbumin-cement composites and hot water-extracted spirulina supernatant cement composites, suggesting that proteins may act as the main hindering agents in the hydration reaction and facilitate protein-related inorganic byproducts. Overall, this study enhances our understanding of the algae-induced hindrance mechanisms on the cement hydration reactions and provides a starting point for improving algae-cements through non-chemical pretreatment on algae biomatter.

TABLE OF CONTENTS

LIST OF FIGURES

LIST OF TABLES

CHAPTER 1 - INTRODUCTION

1.1 CEMENT POLLUTION AND SUSTAINABLE SOLUTION

Concrete, as one of the most commonly used composite materials in modern society, plays a significant role in construction. However, the cement sector, an integral part of concrete production, is recognized as the third largest industrial source of air pollution in the United States, according to the U.S. Environmental Protection Agency.[1] Furthermore, apart from its contribution to global warming potential (GWP) during production, the cement manufacturing process also releases harmful chemicals into the atmosphere, including nitrogen oxides, sulfur dioxide, and carbon monoxide, adversely affecting air quality and human health.[1,2] Addressing these emissions is crucial for creating a more sustainable and environmentally friendly concrete industry. This issue necessitates the exploration of potential solutions.

To combat pollution and reduce the environmental impact of the cement industry, researchers have been actively exploring various approaches for developing the next-generation sustainable cement composite. One promising approach involves the utilization of biomass-based concrete composites to reduce the carbon emissions associated with cement production.[3-5] It includes substituting conventional cementitious materials with organic bio-based alternatives and incorporating natural fibers, such as cellulose, to reinforce the green cement.[6-8]

One of the most extensively studied methods involves the utilization of biomass ash, including biomass bottom ash and biomass fly ash[3,4], as a substitute for clinker, which is the primary carbon emissions component in cement production. While the application of ash has shown promising mechanical properties, some argue that it may not be entirely environmentally friendly due to the combustion process required for ash production, which generates carbon dioxide and other greenhouse gases.

Among the various options for biobased additions, marine algal materials have garnered significant attention. Algae offer several desirable characteristics, including their rapid growth rate and efficient carbon dioxide fixation[8], making them a promising candidate for sustainable materials in various applications. Notably, some literature shows that incorporating brown marine macro-algae into cement composites has demonstrated promising results, showing improvements in (20-30%) compressive strength and a reduction in carbon footprint.[8-12]

However, the same level of success has yet to be observed with micro and green macro algae-based biomatter cement composites, as evidenced by our previous study and the existing literature.[11-13] These particular algae-based composites struggle to meet the desired compressive strength required to meet industry standards in commercial construction.

To address this challenge, this project aims to investigate the underlying factors hindering the hydration reactions of micro and green macro algae-based cement composites. By elucidating the chemical interactions and identifying the specific challenges related to these composites, we can further develop strategies to optimize their mechanical properties and enhance their suitability for sustainable construction practices.

1.2 CEMENT HYDRATION REACTION

To investigate the chemical interaction between algae biomatter and the cement matrix, it is important first to understand the chemical reactions that occur during the typical cement curing process.

The cement powder mixture primarily consists of calcium oxide, calcium hydroxide, silicon dioxide, aluminum oxide, and calcium sulfate. These components are predominantly present as tricalcium silicate (Ca_3SiO_5), dicalcium silicate (Ca_2SiO_4), tricalcium aluminate ($Ca_3Al_2O_6$), tetracalcium ferrite ($Ca_4Al_2Fe_2O_{10}$), and gypsum ($CaSO_4 \cdot 2H_2O$). During the hydration reaction process, various compounds are formed.[14,15]

The main hydration products include calcium silicate hydrate (CSH), calcium hydroxide, calcium aluminate hydrate, and ettringite. Among these, calcium silicate hydrate (CSH) is the primary hydration product that significantly contributes to the mechanical strength of the cement. It is

formed through the hydration reactions of tricalcium silicate (C_3S) and dicalcium silicate (C_2S), which generate calcium hydroxide as a by-product.[14,15] Another important hydration product, although it does not directly contribute to the final compressive strength, is ettringite. It exhibits a distinct morphology (1-5 μm of the prism)[16,17]in the SEM image and serves as an indicator of secondary hydration reactions originating from the hydration of tricalcium aluminate (C_3A).

Understanding the chemical compositions and reactions in the cement hydration process provides a foundation for investigating how algae biomatter interacts with the cement matrix. By examining the changes in these chemical reactions and products, we can gain insights into the influence of algae biomatter on the overall cement performance.

1.3 CHEMICAL COMPOSITION OF MIRCO AND MACROALGAE

This section provides an overview of the two species under investigation in our study: Spirulina sp. and green Ulva sp. Spirulina sp. is a protein-rich blue-green microalgae characterized by spiral-shaped chains of cells and the absence of a hemicellulose cell wall.[18,19] On the other hand, Ulva, commonly known as sea lettuce, is a green macroalgae with an average cell size of 40–50 μm.[20] Ulva primarily consists of polysaccharides with a hemicellulose-based cell wall. By analyzing the fundamental differences in their chemical compositions, we aim to gain insights into the factors contributing to the varying mechanical strengths observed in their respective cement composites.

An examination of the data presented in **Table 1.** reveals significant variations in the reported chemical composition percentages within the same species. This variability can be attributed to factors such as cultivation environment and sub-species variations. However, notable distinctions can still be observed between the two species. Ulva species exhibit higher percentages of carbohydrates and fiber in their raw algae dry mass, while spirulina species predominantly consist of proteins within the dry mass.

Chemical Composition	**Spirulina Species** [25-28]		**Ulva Species** [21-24]	
Carbohydrates And Fiber	10-50%	Monosaccharides: Glucose 20-50% Rhamnose 20-50% Fiber: Hemicellulose 40-50%	40-70%	Monosaccharides: Rhamnose 8-40% Glucose 10-18% Xylose 2-10% Fiber: Hemicellulose 14-21% Lignin 2-10% Cellulose 2-10%
Protein	50-70%	Glutamate Aspartate	4-20%	Aspartate: 10-12% Glutamate: 10-12%
Fatty Acids	1-10%	Palmitic acid: >40%	1-10%	Palmitic acid: 25-50% 18:1n-7: 2-20% α-Linolenic acid: 12-15%
Ash/Mineral	1-7%	Potassium: 640 - 2700 mg/ 100g dry weight Sodium: 450 - 2000mg /100g Iron: 88 mg/100g	3-20%	Magnesium: 3891 mg/100g Calcium: 2720mg/100g Potassium: 630 mg/100 g Sodium: 552 mg/100 g

Table 1. Chemical composition comparison between Ulva sp. and Spirulina sp.[21-28]

1.4 OBJECTIVES

In this study, our objective is to examine the chemical interactions between algae and cement and analyze the variations in compressive strength between micro and macro-algae-based cement composites. Our results reveal a substantial disparity in strength between the (green macroalgae) ulva 5% cement composite samples and (microalgae) spirulina 5% cement composite samples. Significantly, the ulva cement biocomposite demonstrates superior performance compared to the Spirulina cement biocomposites. To address this observation, we propose that a specific chemical component acts as a hindrance agent, impeding the cement hydration process in micro and green macro algae-based composites.

To gain comprehensive insights into the behavior of these cement biocomposites, it is crucial to identify and understand the specific categories of chemical compositions that influence strength and hydration reactions. By investigating representative biopolymer cement composites and modified biomatter cement composites, we can gain valuable insights into the underlying factors that affect strength and hydration processes, enabling us to optimize the performance of cement biocomposites and enhance their potential in sustainable construction applications. Additionally, by studying algae-biomatter extraction, we aim to shed light on the chemical interactions involved.

This investigation into the chemical interaction between algae and cement sets the stage for developing improved algae-based biomatter cement composites, facilitating their successful implementation in commercial construction while meeting industry standards.

CHAPTER 2 – MATERIAL METHODS

2.1 MATERIAL AND CHEMICAL PROCUREMENT

The spirulina was obtained directly from nuts.com, while the ulva seaweed was cultivated in ponds, harvested, and freeze-dried by collaborators from the Pacific Northwest National Labs (PNNL; Sequim, USA). The cement utilized in this study is Type I/II Ordinary Portland Cement (Sakrete, Atlanta, GA).

2.2 CEMENT COMPOSITE SAMPLE-MAKING PROCESS

2.2.1 Cement casting mold

The reverse mold utilized in this study is created using a 3D printer and PLA plastic material. The rubber mold employed for casting the cement samples is produced by filling the reverse mold with VytaFlex urethane rubbers (Smooth-On, Macungie, PA). To comply with the capacity

limits of our compression test frame, two different dimensions of molds ($10mm^3$ and $8mm^3$) were employed to manufacture the cement composite samples.

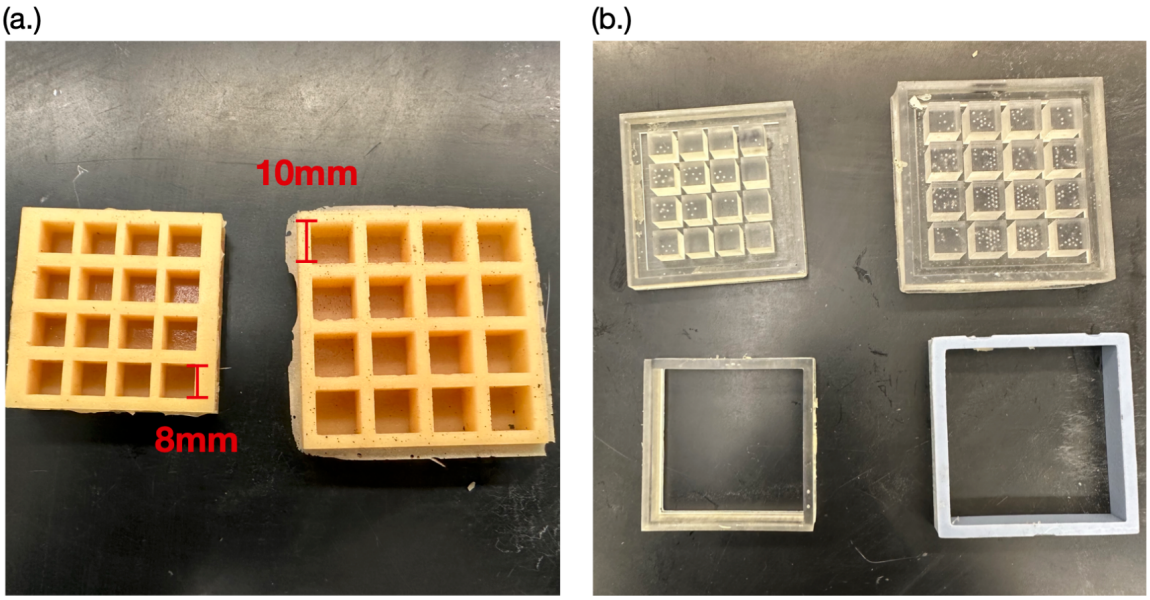

Figure 1. (a.) Rubber mold for cement samples. (b.) Reverse mold for casting the rubber mold.

2.2.2 Biomatter grinding process

To provide sufficient surface area for chemical reactions between biomass and cement, desired amount of biomatter was ground using an electric coffee grinder for 30 seconds. This grinding step ensured the biomass was finely powdered and ready for subsequent procedures. In the case of Spirulina, the extraction methods were executed using the powder directly obtained from the packaging without any additional processing steps.

2.2.3 Cement mixing process

When incorporating solid biomatter powder into cement, the process involves pre-mixing Portland Cement powder with dry biomatter powder to achieve a homogeneous powder mixture. Subsequently, the mixture is mixed with water for 180 seconds, using a four times 45-second mixing period with a 15-second resting intervals session for producing the cement slurry.

Sample casting is carried out by manually pouring the cement slurry into a rubber mold placed on a vibration table, aided by a thin metal spatula. Once the rubber mold is filled, a transparent plastic film is placed on top to secure the slurry. The filled mold is then transferred to an enclosed chamber with a relative humidity of approximately 85%, where it undergoes curing until the desired testing date.

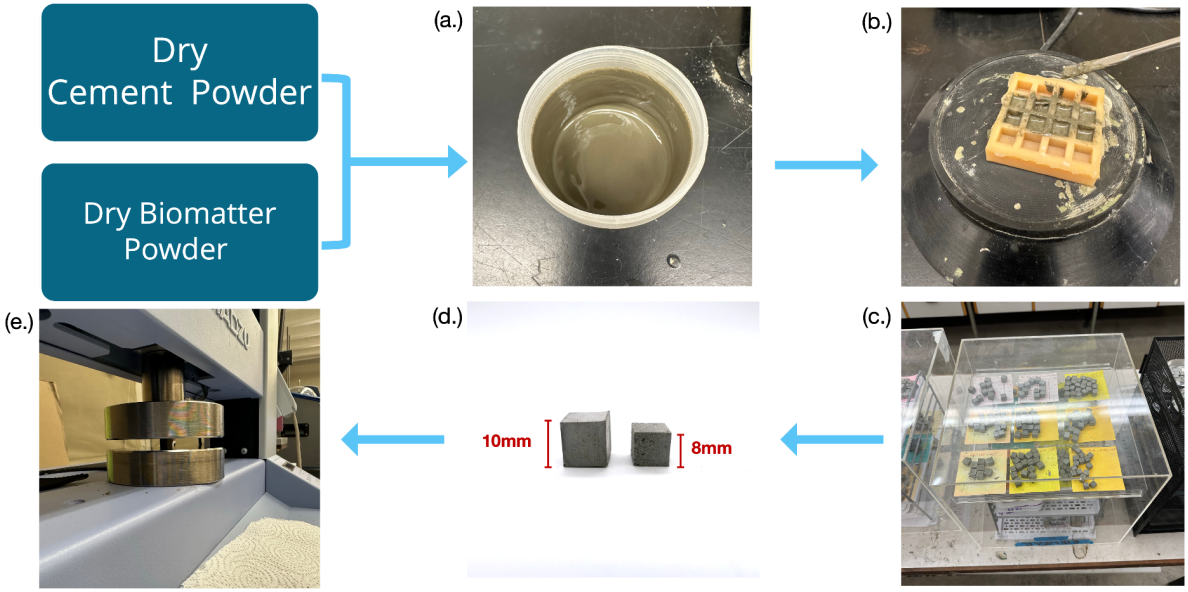

Figure 2. Diagram of sample-making process. (a.) Cement slurry after mixing with water. (b.) Sample casting process on the vibrational table. (c.) Curing stage (d.) $10mm^3$ and $8mm^3$ individual samples (f.) Mechanical testing.

2.3 EXTRACTION METHODS

2.3.1 Literature Study On Extraction Procedure And Process

The extraction procedure for this study was determined through a modified version after conducting several literature reviews. Chaiklahan et al. [29] reported the optimal conditions for Spirulina extraction, including a solid-to-liquid ratio of 1:45 (w/v) Spirulina to water, a temperature of 90°C, and a duration of 120 minutes, resulting in a biomass yield of 8.3% dry weight. Yongzhou Chi et al. [30] found that a ratio of 1:30 algae to water, an extraction temperature of 100°C, and a duration of 2 hours yielded successful results for Ulva species. Additionally, MyoungLae Cho et al. [31] reported that an algae-to-water ratio of 1:20, an extraction temperature of 65°C, and a duration of 2 hours, with constant mechanical stirring, provided satisfactory outcomes. However, it is important to note that in our study, we did not execute the deportation and lipid removal procedures as described in the aforementioned literature. Consequently, the extracted supernatant likely contains multiple types of biopolymers.

The reason for conducting both hot water and cold water extractions is to investigate the effects of different extraction temperatures on the composition of biomass cement. In the case of hot water extraction, the goal is to extract a maximum amount of water-soluble substances by utilizing heat to break down the cell walls of the biomass. This method allows us to examine the

impact of heat on the composition of the biomass and observe any changes in the cement properties.

On the other hand, cold water extraction allows for a direct comparison of the effects of heat on the biomass. By conducting the extraction process without applying heat, we can maintain the protein in its native form and evaluate the specific influence of temperature on the composition of the biomass. This approach also enables us to observe the potential effect of protein denaturation. Hence, by employing both hot and cold water extraction methods, we aim to gain comprehensive insights into the effects of temperature and extraction procedures on the composition of biomass cement.

2.3.2 Polysaccharides Hot-water extraction (HWE)

The hot water extraction (HWE) process of algae in the study involved specific parameters. A 1:30 (w/w) ratio solution was prepared between the algae biomass and water during extraction. The procedure was carried out at 100°C for 2 hours. To compensate for water evaporation, one-third of the initial weight of the water was added after the first hour of extraction, ensuring a consistent liquid environment. After completion of the extraction process, the mixture was allowed to cool down to room temperature. Subsequently, centrifugation was performed at 6000 rpm for 10 minutes to separate the solid biomass from the liquid extract, ensuring the isolation of the desired components.

2.3.3 Polysaccharides Cold-water extraction (CWE)

A 1:30 (w/w) ratio solution was prepared between the algae biomass and water during extraction. The procedure was carried out at room temperature for 24 hours. After completion of the extraction process, centrifugation was performed at 6000 rpm for 10 minutes to separate the solid precipitate and the liquid supernatant.

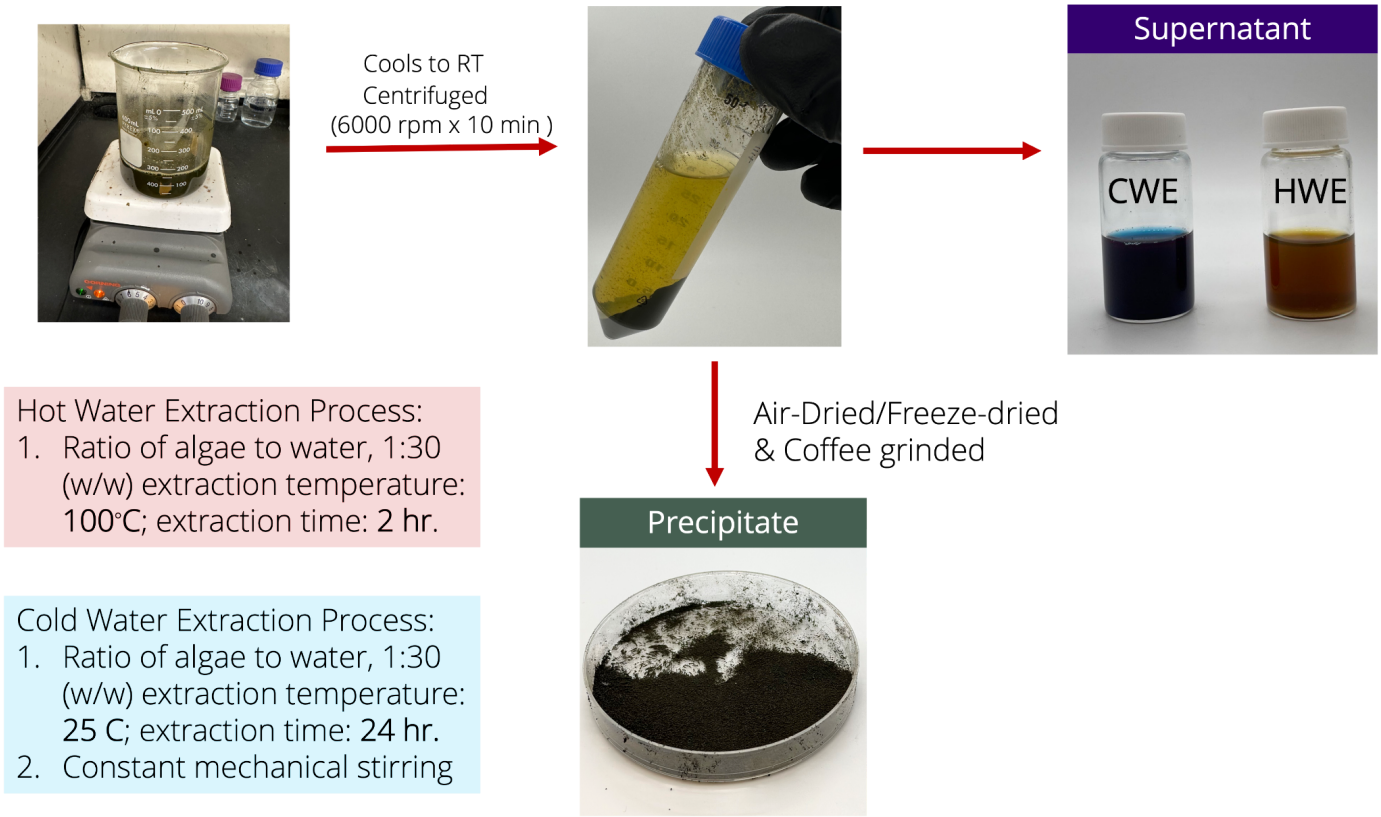

Figure 3. Diagram of the extraction procedure

2.3.4 Sample-Making Process for Extraction Product

The sample-making process for the extraction precipitate involved the following steps. First, the precipitate obtained from the centrifuged solution was air-dried. Once the precipitate was completely dried, a coffee grinder was used to grind it into a fine powder. Subsequently, the standard process for making cement composite samples was followed to produce the testing sample.

And for the supernatant cement composite samples, after the supernatant was collected, the supernatant was incorporated into the cement during the sample-making process, serving as the water component.

2.4 PROTEIN ENVIRONMENT STUDY

2.4.1 Cement Pore Water Preparation

The cement pore water used in this study is prepared by mixing cement powder with desired water-to-cement ratio using a four times 45-second mixing period with a 15-second resting intervals session with a total of 180 seconds of mixing time. After the mixing process, centrifugation was performed at 6000 rpm for 10 minutes, and the cement pore water was collected.

2.4.2 Lactalbumin Sample Preparation

For the lactalbumin sample, we mixed 1g of alpha-lactalbumin dry powder with 20g of the desired solution. The mixture was left overnight and then subjected to the freeze-drying procedure.

2.4.3 Freeze Drying Procedure

The Protein Environment Study involved the freezing of lactalbumin solution using liquid nitrogen, followed by loading the samples into a freeze-drier for 48 hours to ensure complete drying. The specific freeze-drier used in this study was the FreeZone 2.5 Liter -50C Benchtop Freeze Dryer from Labconco, which provided the conditions for the freeze-drying process. By employing this freeze-drying technique, the samples were effectively preserved and prepared for further analysis in a dry state, facilitating the investigation of the protein denaturation study.

2.5 CHARACTERIZATION METHODS

2.5.1 Compression Test

The testing is done with Shimadzu Autograph AGS-X Series Universal Tester (Load cell maximum limit: 5kN). Cement composite samples are tested on day 3, day 7, day 14, and day 28 to see the compressive strength evolution.

Before conducting the compression test, the cement samples were carefully demolded. To ensure a more even surface, 400-grit sandpaper was used to smooth the sample surfaces. The dimensions of each sample were measured using a caliper, while the weight was determined using a digital scale. Subsequently, the samples were loaded onto the test frame, ensuring proper alignment. The compression test was performed with a speed of 13.73 $N/mm^2/min$, and the load was limited to 5 kN.

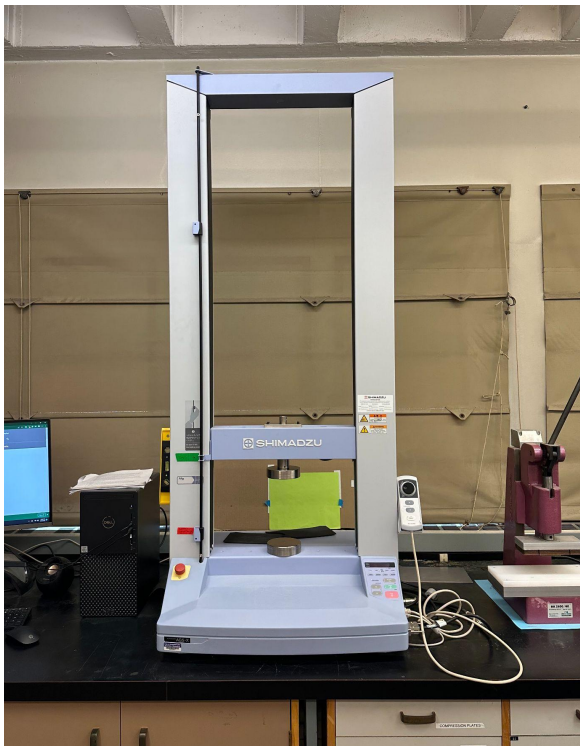

Figure 4. Shimadzu Autograph AGS-X Series Universal Tester was used in this study for compression testing.

2.5.2 Scanning Electron Microscopy And Energy-dispersive X-ray Spectroscopy

Scanning Electron Microscopy (SEM) allows us to examine the morphology of the various cement composite matrix and identify the hydration product and nanofiber produced to verify the hypothesis. SEM samples were sputter coated with gold particles on SC7620 from Quorum Technologies. The SEM used in this study is JEOL JSM-6010 Plus from the University of Washington Material Science and Engineering Department and Phenom ProX SEM from Washington Clean Energy Testbeds.

Energy-dispersive X-ray spectroscopy (EDS) was employed to investigate the elemental composition of the samples by analyzing the unique characteristics exhibited when X-rays interact with different atomic structures. The EDS test was performed using a Phenom ProX scanning electron microscope (SEM) at the Washington Clean Energy Testbeds.

2.5.3 Thermogravimetric Analysis

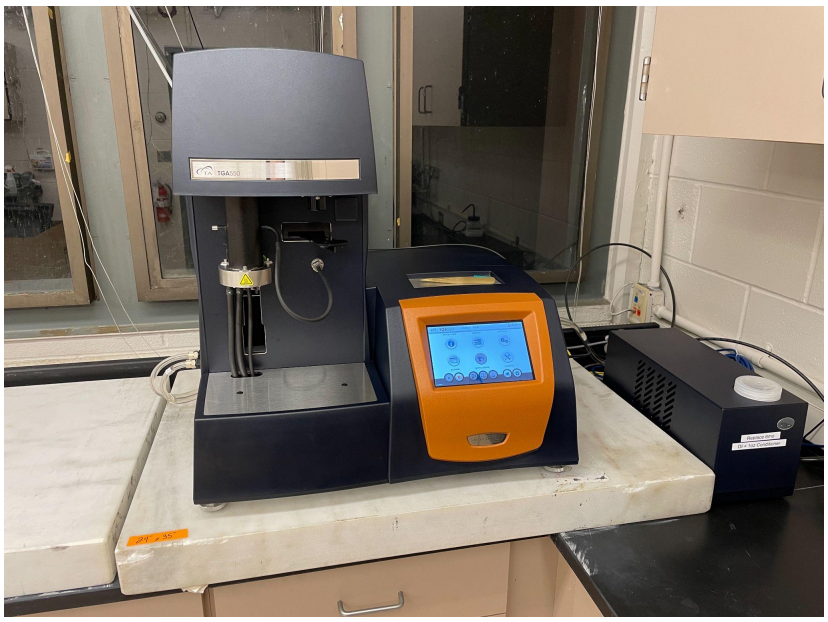

Figure 5. TGA 550 Discovery from TA Instruments used in this study for thermogravimetric Analysis

Thermogravimetric Analysis (TGA) could monitor the mass change as a function of the selected heating profile. In cement matrix, the typical thermogravimetric analysis (TGA) decomposition curve shows three main regions: the loose-bonded water desorption region from room temperature to 140°C, the calcium hydroxide decomposition region from 380°C to 520°C, and the calcium carbonate decomposition region from 650°C to 800°C [32,34,35]. In our study, we will focus on the calcium hydroxide decomposition region, as this region is crucial for understanding the strength contribution of the primary hydration product in the cement matrix, and it exhibits a distinct drop that allows for easy qualitative comparison.[34,35] The heating profile of cement composite used in this study consists of heating up to 140°C with a heating speed of 10°C/ min and then holding isothermal at 140°C for 25min. Subsequently, use the

same heating speed to reach 1000°C and hold it for 30min to ensure all the materials have been burnt off and left with accurate ash content. Additionally, for the water content test for extraction supernatant, the heating profile consists of slowing heating up to 90°C using 1°C/ min heating speed and holding it for 120min after reaching 90°C to ensure all the water has been fully evaporated. And subsequently heated to 700°C and held for isothermal for 30min to ensure an accurate ash content. This study performs the TGA test using TGA 550 Discovery from TA Instruments.

2.5.4 Fourier-transform infrared spectroscopy

Fourier-transform infrared spectroscopy (FTIR) enables observing chemical interactions between functional groups by examining the shift in vibration peaks. This analysis used a Thermo Scientific iS10 Nicolet FTIR instrument at the Washington Clean Energy Testbeds. Each spectrum was recorded within the range of 7800–350 cm^{-1}, utilizing a resolution of 2 cm^{-1} over 64 runs.

CHAPTER 3 – RESULTS AND DISCUSSION

3.1 ANALYSIS OF BIOPOLYMER ADDITIVE CEMENT COMPOSITE

The Spirulina and Ulva species under investigation comprise four primary chemical components: polysaccharides, disaccharides, lipids, and proteins. To assess the impact of these components on cement composites, representative chemicals were selected for each category based on accessibility and functional group characteristics. Specifically, glucomannan was chosen to represent polysaccharides, sucrose for disaccharides, stearic acid for lipids, and lactalbumin for proteins. In this analogous study, cement composites containing 5% of each representative chemical will be compared with those containing 5% of Spirulina and Ulva, respectively, using a water-to-cement (w/c) ratio of 0.4. The behavior of these composites will be evaluated through compression tests, thermogravimetric analysis (TGA), and scanning electron microscopy (SEM) imaging.

Prior to incorporating the selected biopolymer into the cement matrix, we conducted particle size distribution (PSD) analysis and examined the morphology of the biopolymer using scanning electron microscopy (SEM) imaging. The purpose of the PSD analysis was to ensure that the particle size of the biopolymer was within an appropriate range, as excessively large particles could introduce defects in the cement matrix and impede the observation of the chemical reaction effects when the biopolymer is insoluble. We presented the particle size distribution of lactalbumin and stearic acid, with average particle sizes of 15.998 μm and 20.79 μm, respectively. These sizes are comparable and suitable for investigating the chemical influence. Additionally, SEM imaging enabled us to visualize the morphology of the biopolymer outside the cement matrix.

3.1.1 Mechanical Properties

The mechanical testing results for cement composites containing 5% of each representative chemical, as well as 5% of spirulina (SP5), ulva (UV5), and their respective controls, are presented in **Figure 7a**. The data indicate that glucomannan and lactalbumin at 5% concentration had the most detrimental impact on the final strength of the composites. By adding 5% glucomannan (GM5), the compressive strength at day 28 decreased from 57.17 ± 4.19 MPa to 2.07 ± 0.31 MPa while it decreased from 57.17 ± 4.19 to 8.52 ± 0.60 MPa when introducing 5% lactalbumin. In contrast, stearic acid 5% (SA5) and sucrose 5% (SU5) had a similar final strength to the Ulva 5% (UV5) samples (in the range of 25-30 MPa, 44-52% of pure cement). These results suggest that proteins and polysaccharides may be the primary factors contributing to the cement's weaker mechanical strength and hindrance of hydration.

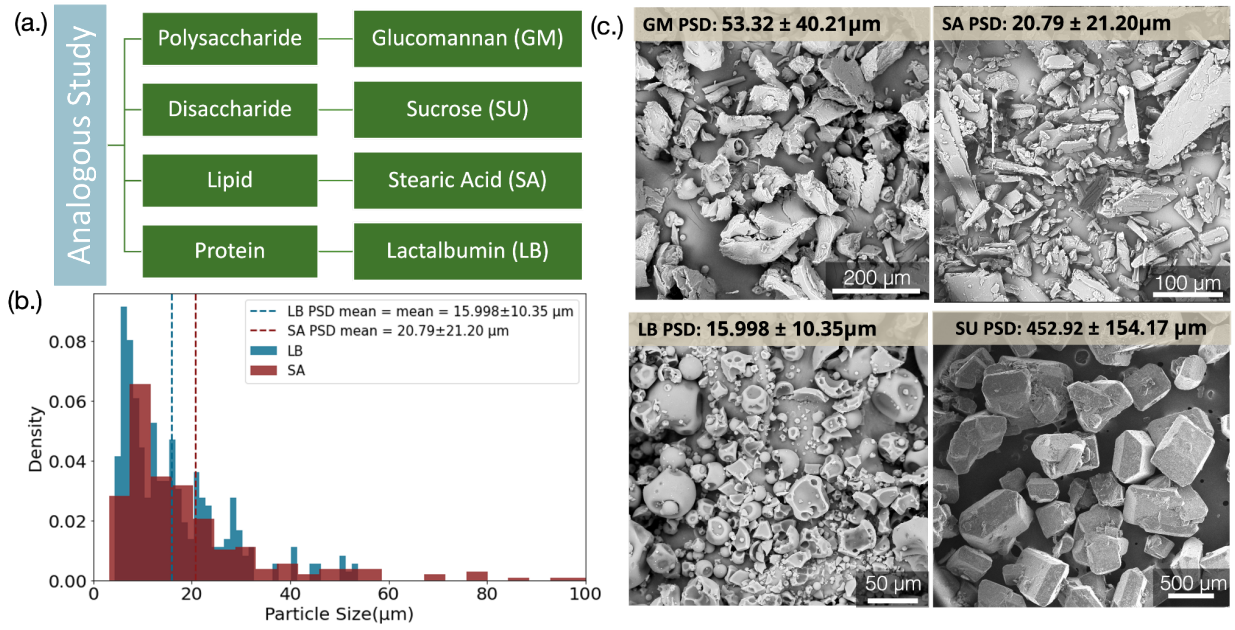

Figure 6. (a.) Schematic diagram of biopolymer additive for analogous study. (b.) Particle size distribution of biopolymer additive (c.) SEM images of biopolymer additives

Next, we investigated the hydration products by looking at the TGA curve of analogous cement composites and comparing them with the degradation regions of typical cement hydration products. In **Figure 7b.**, the pure cement (PC) and Ulva 5% cement composite (UV5) exhibit a typical calcium chloride (CH) decomposition drop in the TGA result, which is around 380°C to 520°C area in the figure.[32,34,35] The absence of calcium chloride alines with compressive strength results where the two composites are stronger than most others. Interestingly, although the strength of SU5 is similar to the UV5, it does not show a typical calcium chloride ($Ca(OH)_2$) decomposition drop in the TGA curve, suggesting that the sucrose 5% composite's strength might not be contributed by the typical hydration products.

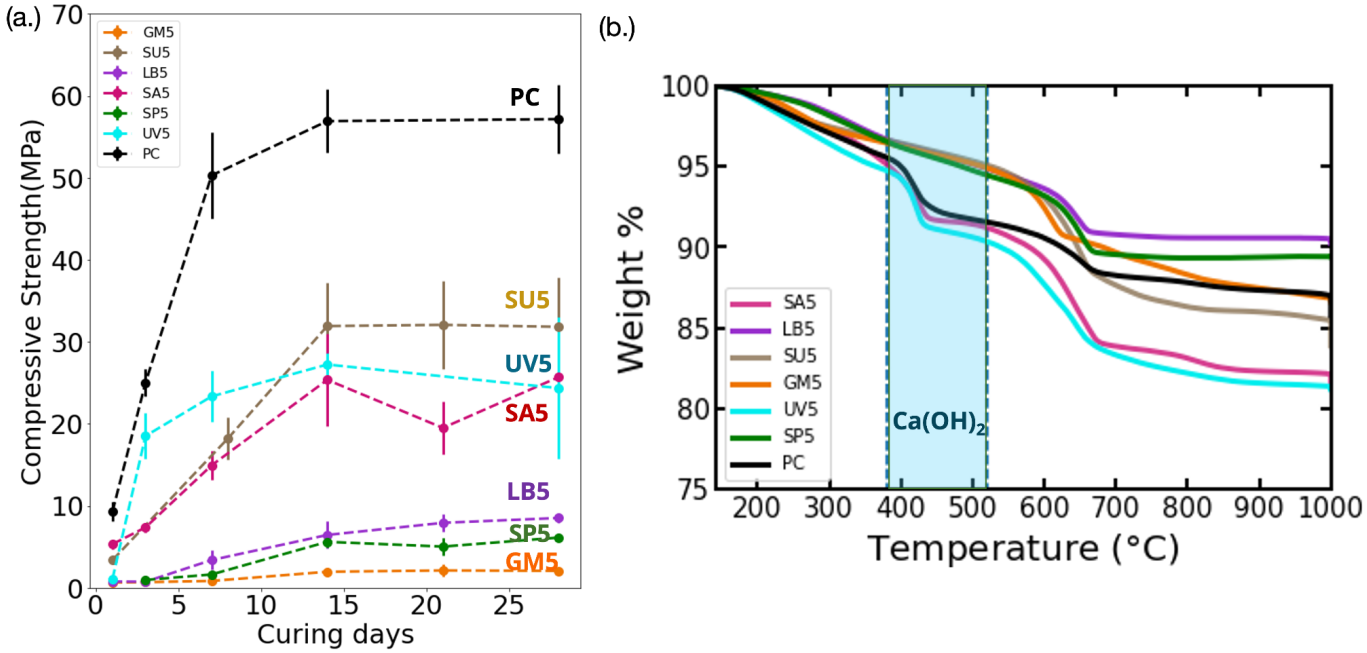

Figure 7. (a.) Compression test result for biopolymer additive cement composite compares to pure cement(PC), Ulva 5% cement composite (UV5), and Spirulina 5% cement composite (SP5). (b.) TGA result for biopolymer additive cement composite compared to PC, UV5, and SP5

3.1.2 Morphological Analysis

The scanning electron microscopy (SEM) images further support the findings of the thermogravimetric analysis (TGA), illustrating a remarkably dense and well-bonded matrix, as shown in **Figure 8a.** In the stearic acid 5% cement composite (SA5), sintered CSH plate-like structures and ettringite needles are observed within the matrix. This observation aligns with the TGA results, which indicate a drop in $Ca(OH)_2$ decomposition, indicating the presence of typical hydration products.

Notably, unlike typical cement hydration products such as ettringite needles, an intriguing observation in the lactalbumin 5% cement composite (LB5) is the significant occurrence of distinct nanofibers at a similar scale. (**Figure 8b.**) These nanofibers are suspected to be distinct products from an alternative chemical reaction. To gain further insights into the composition of these nanofibers, we employed energy-dispersive X-ray spectroscopy (EDS) for the comprehensive characterization of the composites.

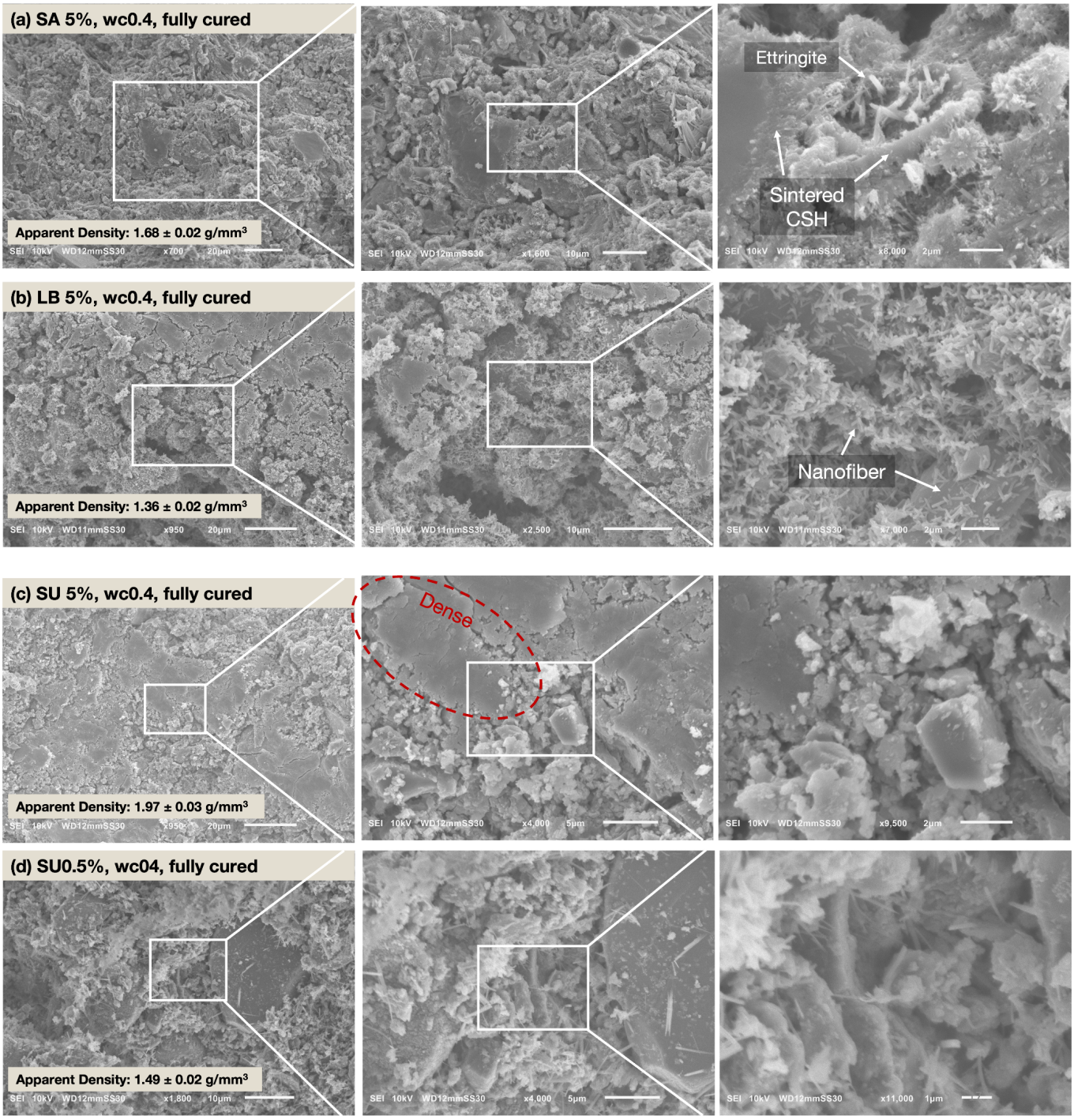

Figure 8. SEM image of biopolymer additive composite. (a.) Stearic acid 5% cement composite, w/c = 0.4, fully cured, with an apparent density of 1.68 ± 0.02 g/mm^3(b.) Lactalbumin 5% cement composite, w/c = 0.4, fully cured, with an apparent density of 1.36 ± 0.02 g/mm^3(c.) Sucrose 5% cement composite, w/c = 0.4, fully cured, with an apparent density of 1.97 ± 0.03 g/mm^3(d.) Sucrose 0.5% cement composite, w/c = 0.4, fully cured, with an apparent density of 1.49 ± 0.02 g/mm^3

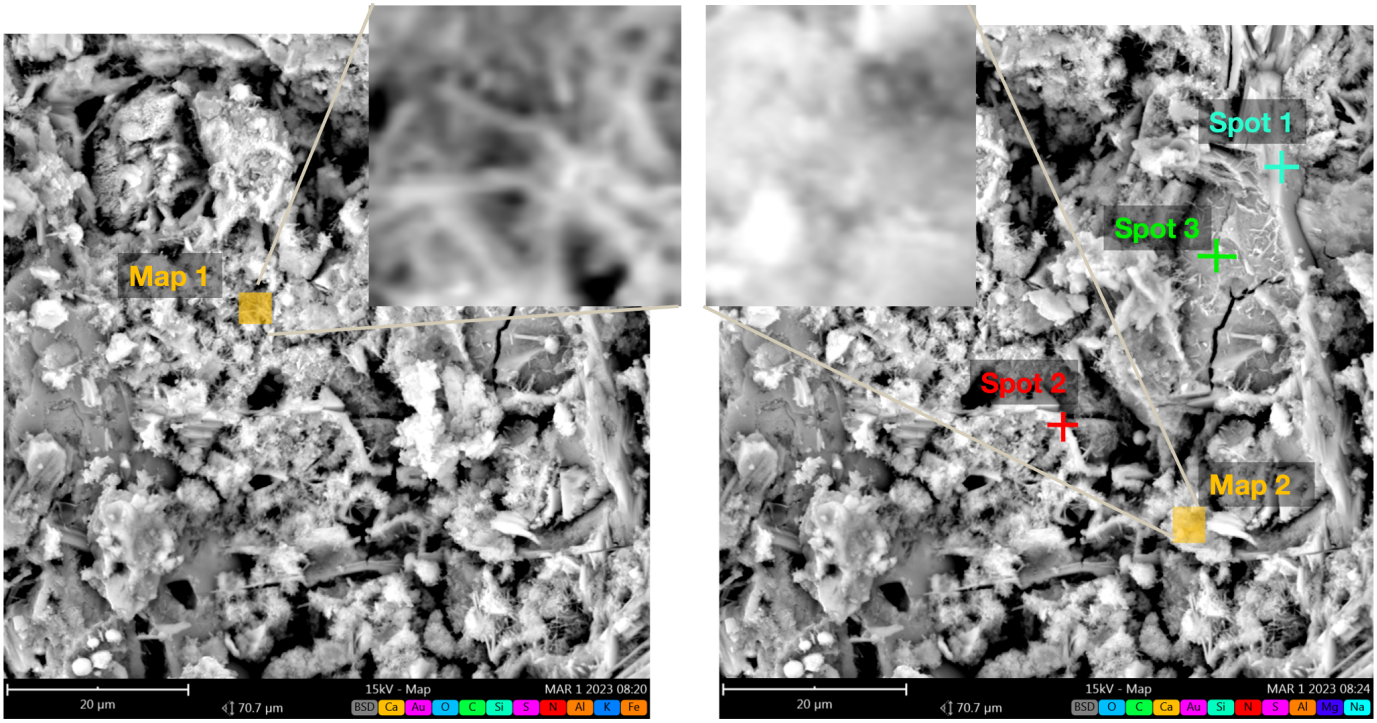

Figure 9. Composition profile of 5% glucomannan cement composite.

Element Symbol	Map 1 Atomic Conc. Nanofiber	Map 2 Atomic Conc. Nanofiber	Spot 1 Atomic Conc. Densified Matrix	Spot 2 Atomic Conc. Densified Matrix	Spot 3 Atomic Conc. Densified Matrix
O	36.35	47.30	49.14	27.40	20.73
C	9.36	24.84	15.22	6.47	5.09
Ca	36.82	17.15	24.30	49.69	60.25
N	2.18	2.14	2.96	2.67	2.66
Si	7.24	4.17	4.58	7.25	6.92
S	4.15	1.62	1.21	1.52	2.12
Al	1.63	1.09	1.56	0.80	0.44
Ca/Si ratio	5.09	4.11	5.31	6.85	8.71

Table 2. Elemental ratio of 5% glucomannan cement composite

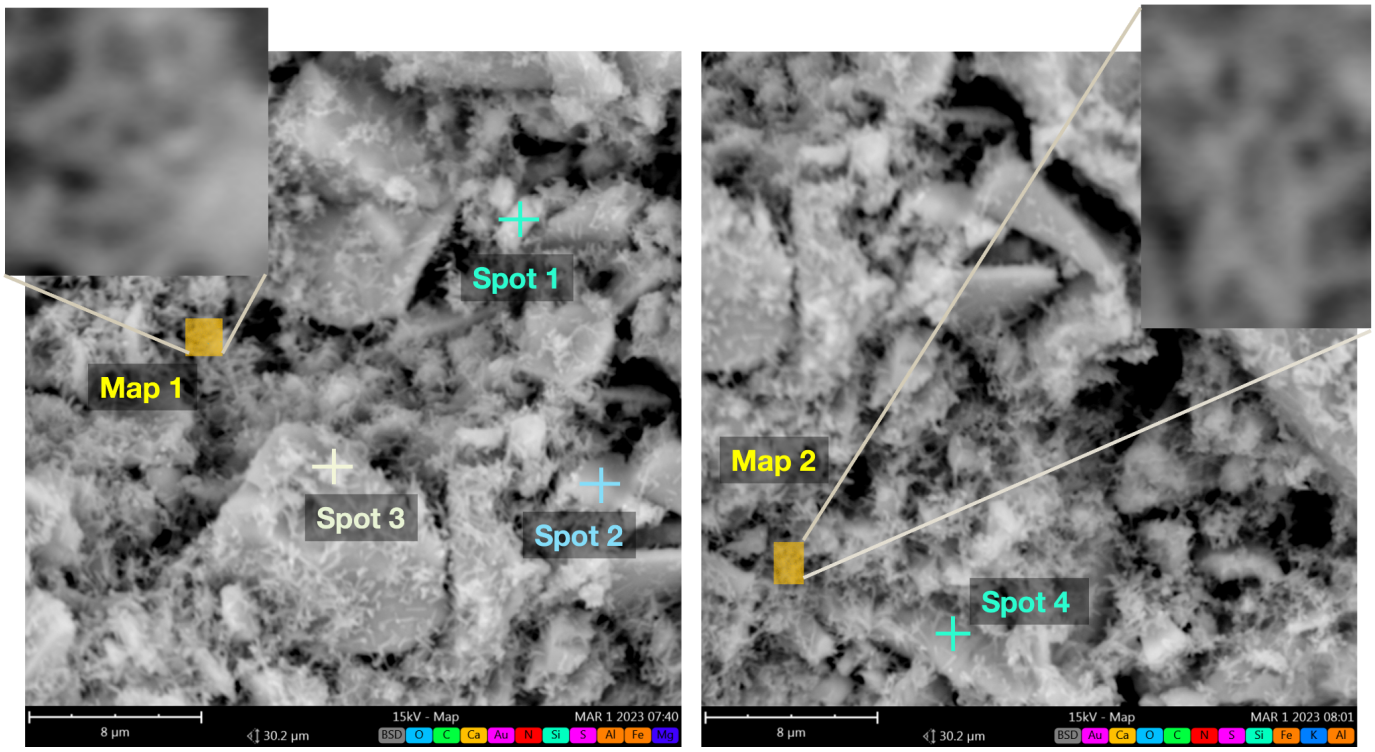

Figure 10. Composition profile of 5% lactalbumin cement composite.

Element Symbol	Map 1 Atomic Conc. Nanofiber	Map 2 Atomic Conc. Nanofiber	Spot 1 Atomic Conc. Nanofiber	Spot 2 Atomic Conc. CSH	Spot 3 Atomic Conc. CSH	Spot 4 Atomic Conc. Densified Matrix
O	53.15	20.97	29.95	58.51	55.43	26.85
C	19.21	11.87	11.76	14.29	19.21	11.89
Ca	15.37	56.02	41.78	11.82	12.53	49.30
N	3.74	3.28	5.84	5.30	4.68	7.67
Si	2.91	2.02	7.23	6.87	4.96	1.50
S	2.61	2.80	1.42	1.16	0.71	0.77
Al	1.32	0.41	0.58	0.71	0.78	0.43
Ca/Si ratio	5.28	27.73	5.78	1.72	2.53	32.87

Table 3. Elemental ratio of 5% lactalbumin cement composite

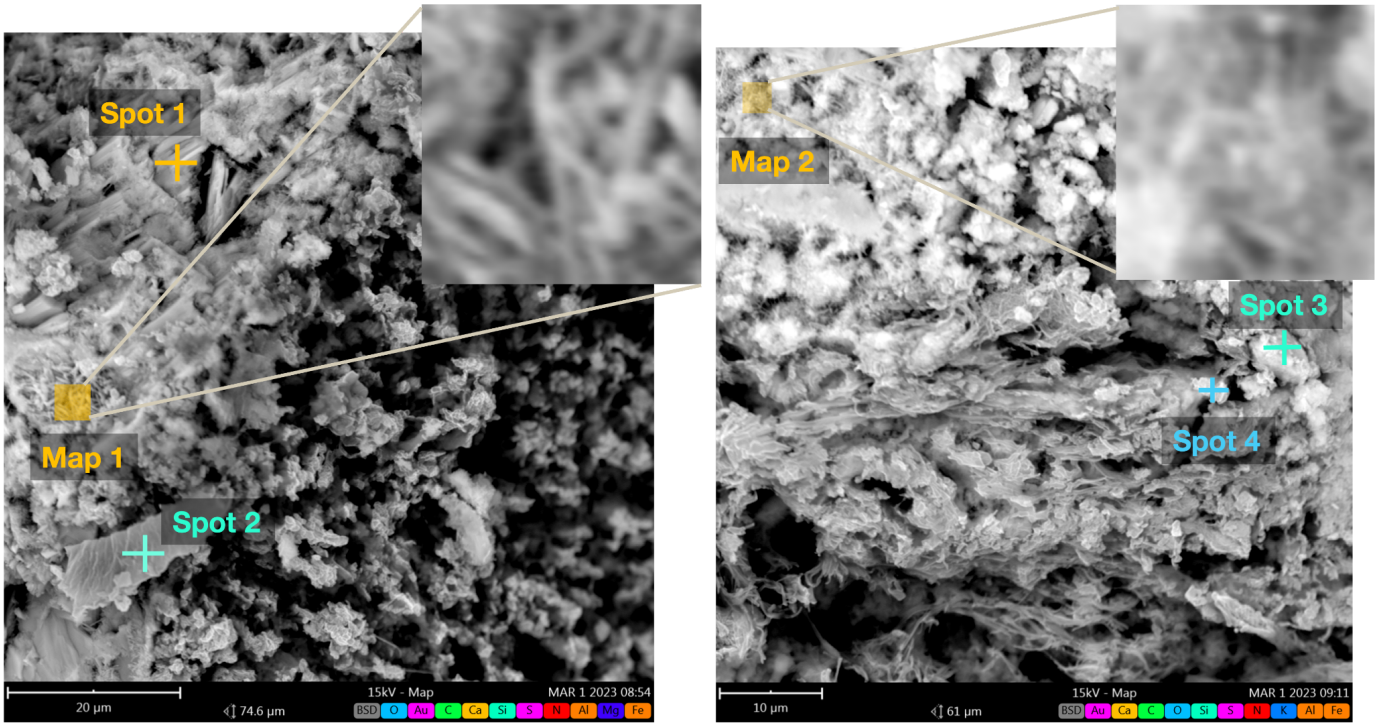

Figure 11. Composition profile of 5% Stearic acid cement composite.

Element Symbol	Map 1 Atomic Conc. Nanofiber	Map 2 Atomic Conc. Nanofiber	Spot 1 Atomic Conc. Densified Matrix	Spot 2 Atomic Conc. Densified Matrix	Spot 3 Atomic Conc. CSH	Spot 4 Atomic Conc. Nanofiber
O	45.38	14.39	63.01	3.22	52.08	13.23
C	17.31	24.53	N/A	95.67	26.24	74.15
Ca	21.94	49.08	23.31	0.40	11.19	8.21
N	1.88	1.69	5.23	0.26	2.75	0.81
Si	4.42	6.11	5.04	0.12	5.74	1.49
S	4.09	2.38	0.95	0.07	0.62	1.01
Al	1.88	0.58	0.95	0.06	0.83	0.38
Ca/Si ratio	4.96	8.03	4.63	3.33	1.95	5.51

Table 4. Elemental ratio of 5% stearic acid cement composite.

3.1.3 Elemental Composition Of Nanofiber

EDS was employed to investigate the elemental composition of the microstructure and correlate it with the hydration products, providing insights into the chemical reactions between the filler and cement matrix. (**Table 2., 3.,** and **Table 4.)** reveals that the Ca/Si ratio is higher in all the representative cement composites. The unhydrated cement components belite and alite have theoretical Ca/Si ratios of 2 and 3, respectively, and the Ca/Si ratio of 0.6-2.6 for CSH, a typical Portland cement hydration product, is reported in previous studies.[35-37] A different nanofiber in the representative cement matrix, distinct from the typical Ca/Si ratio value of cement hydration products, is observed in the range of 1–5 μm[35] (see **Table 2. 3., and 4.)**. The glucomannan (**Figure 9., Table 2.**) and stearic acid (**Figure 11., Table 4.**) cement composite analysis show a higher carbon content, corresponding to the long-chain carbon backbone of both the biopolymers. Meanwhile, the lactalbumin 5% (**Figure 10., Table 3.**) cement composite data shows a significantly higher amount of nitrogen content across all analysis points than the glucomannan and stearic acid cement composite results, suggesting the presence of proteins. Additionally, torpedo-shaped nanoparticles with an extremely high Ca/Si ratio might be a unique product derived from the protein-cement interactions. The identifiable CSH products in the lactalbumin composite in the EDS result explain its better compressive strength than the glucomannan composite.

3.2 SACCHARIDE RETARDATION STUDY

Comparing the influence of disaccharide and polysaccharide on the compression strength of the composites, it is evident that the SU5 cement composite exhibits better than expected compressive strength, while the GM5 composite shows significantly weaker mechanical properties. However, this difference could be attributed to the extreme water uptake ability of glucomannan which would become a viscous hydrogel upon meeting water and decrease the workability of the slurry, leading to a noticeable amount of manufacturing voids.[33] To further exclude the influence of workability-induced defects on the compressive strength, lower percentages (0.5%) of sucrose and glucomannan were added to the cement composite.

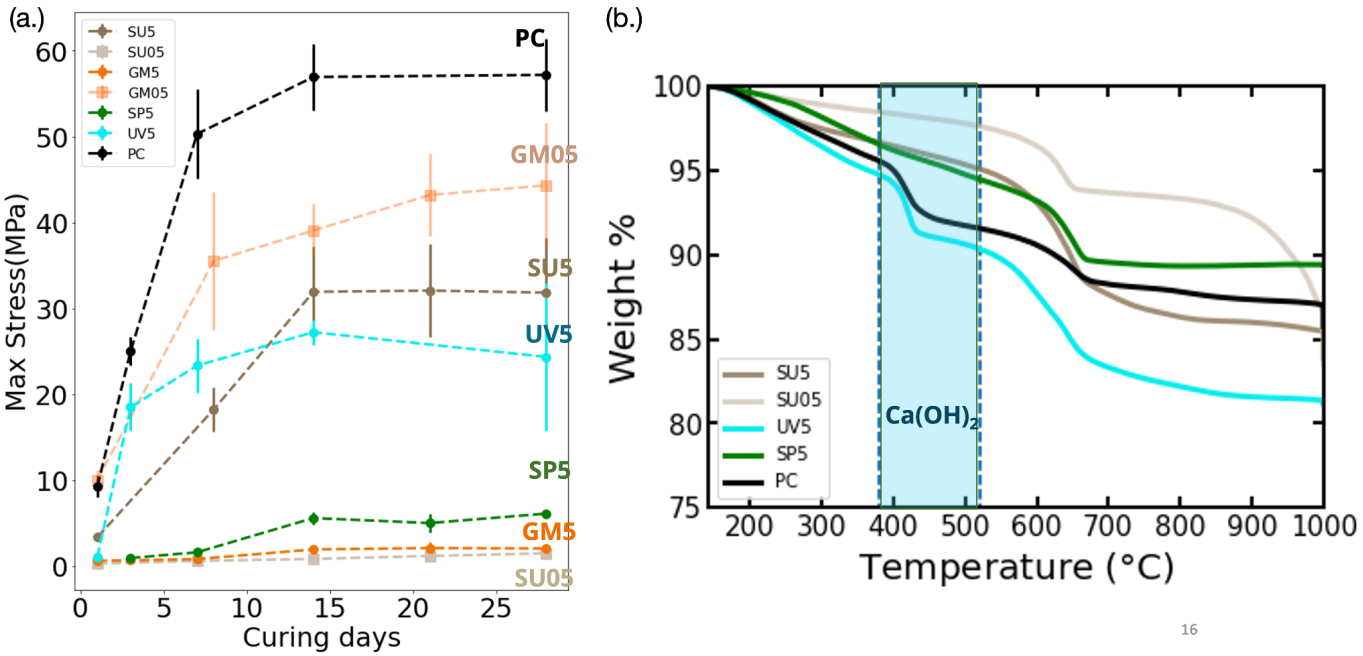

Figure 12. (a.) Compression test results for sucrose 5% and 0.5% cement composite and glucomannan 5% and 0.5% compared to pure cement (PC), Ulva 5% cement composite (UV5), and Spirulina 5% cement composite (SP5). (b.) TGA result for sucrose 5% and 0.5% cement composite compare to PC, UV5, and SP5

We compare the compressive strength between the 0.5% sucrose cement composite (SU05) and the 0.5% glucomannan cement composite (GM05) as shown in **Figure 12a.** Interestingly, the results reveal that GU05 outperforms SU05 in compressive strength, indicating that the lower molecular weight of saccharide has a more destructive influence on the strength at the same percentage. Additionally, we find an interesting relationship between the sucrose concentration and the final compressive strength. Contrary to our previous notion that incorporating more retardants into the cement matrix would lead to lower mechanical properties, SU05 exhibits lower mechanical strength than SU5 while both samples do not show a typical $Ca(OH)_2$ decomposition at 380-520℃ (**Figure 12b.)**, implying the hindrance of primary hydration reaction derived from alite and belite.

To further validate the results obtained from the mechanical testing, we conducted scanning electron microscopy (SEM) analysis on the SU5 and SU05 cement composites. Upon examining the SEM images from **Figure 8c.** and **Figure 8d.**, the SU5 composite exhibits a denser matrix than the SU05 composite, correlating to the higher apparent density of the SU5 composite (~1.97 g/mm^3). The denser matrix in the SU5 composite contributes to its superior mechanical properties, as confirmed in the compressive strength results. To be noted, we observe the ettringite needles (1.35 ± 0.01 μm) in the SU05 matrix, which is not observed in the SU5 matrix. The higher compressive strength and denser matrix may attribute to the sucrose crystalization and reinforcing the matrix. The higher compressive strength and denser matrix in the SU5 composite may be attributed to sucrose crystallization and reinforcement of the matrix.

However, the exact cause of this phenomenon remains unclear and warrants further investigation using X-ray diffraction (XRD). The differences in microstructure and morphology between the two composites contribute to the variations in their mechanical properties. Further research is needed to fully understand the mechanisms behind these observations.

3.3 ANALYSIS OF EXTRACTION-MODIFIED ALGAE CEMENT COMPOSITE

3.3.1 Mechanical Properties

Upon finding that polysaccharides and proteins are the primary components responsible for the retardation and hindrance of the cement hydration process, we applied extraction methods to remove these undesirable components and improve the performance of the algae biomatter cement composite. Extraction modification of raw algae material holds great potential for enhancing the low performance of raw algae cement composites. In this study, we performed hot and cold water extractions on micro and macroalgae, specifically spirulina and ulva. These extraction methods were selected for their environmentally friendly nature, as they require less intensive chemical pretreatment and result in lower carbon footprints compared to other methods requiring multistep chemical treatment and drying processes.

We incorporated the obtained biomass precipitate into 5% cement matrices with a water-to-cement ratio of 0.4 (w/c) to compare its performance with the raw algae cement

composite directly. Additionally, we incorporated the resulting supernatant into cement composites to evaluate its effect compared to pure cement. The performance of these composites was evaluated through compression tests, thermogravimetric analysis (TGA), and scanning electron microscopy (SEM) imaging.

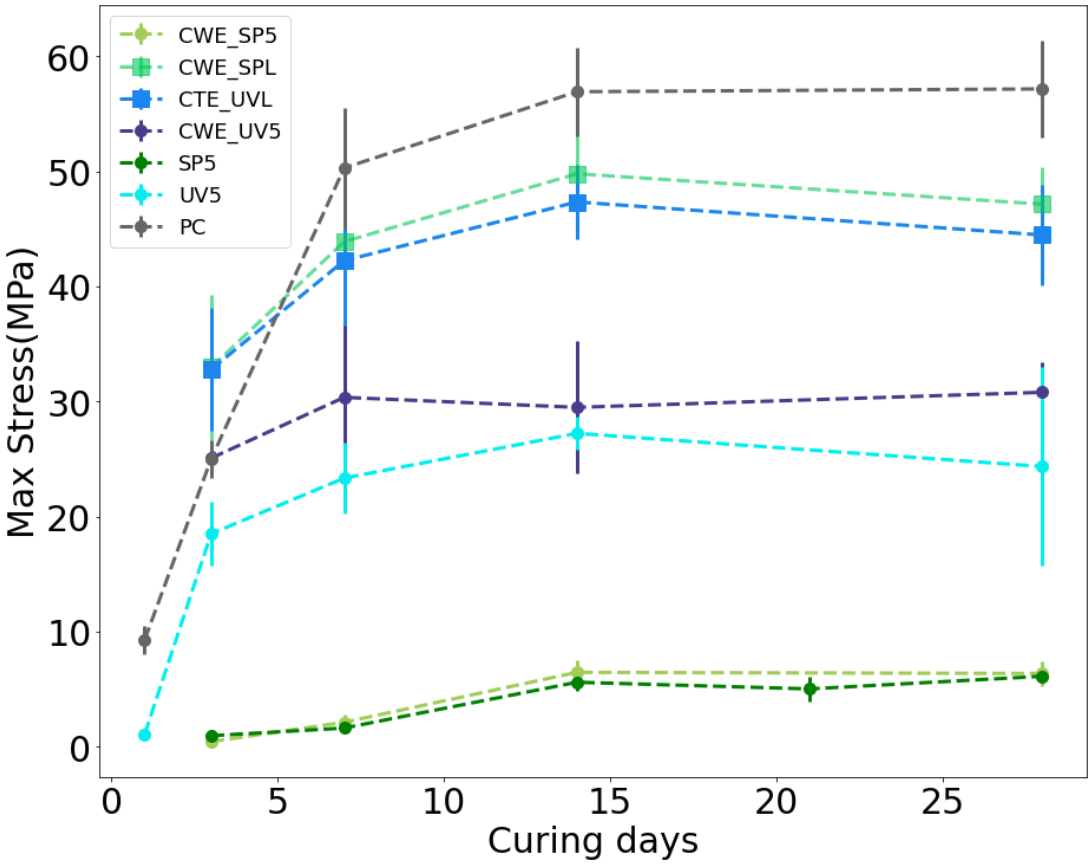

Figure 13. Compression test result for cold water extracted spirulina precipitate solid 5%(CWE_SP5) and supernatant liquid (CWE_SPL) cement composite, Cold water extracted ulva precipitate solid 5% (CWE_UV5) supernatant liquid (CWE_UVL) cement composite and compare to PC, UV5, SP5.

Comparing the compressive strength of the composites with 5% virgin biomass and pretreated biomass, as shown in **Figure 13.**, we find that the cold water extracted Ulva precipitate solid 5% cement composite (CWE_UV5) demonstrates slightly superior performance compared to its virgin counterparts by 20.6%. Conversely, the cold water extracted spirulina precipitate solid

5% cement composite (CWE_SP5) exhibits a similar compressive strength to SP5 while CTW_SPL shows a slight decline in compressive strength. The combined results from the compressive strength of spirulina supernatant and precipitate composites derived from the cold water extraction suggest that the cold water extraction method alone is insufficient to remove the detrimental components from virgin spirulina. Consequently, we employed more effective hot water extraction methods [29-31] to investigate this matter further.

Next, we compared algae cement composite modified by the hot water extraction method with raw ulva, spirulina cement composite, and pure cement. (**Figure 14.**)

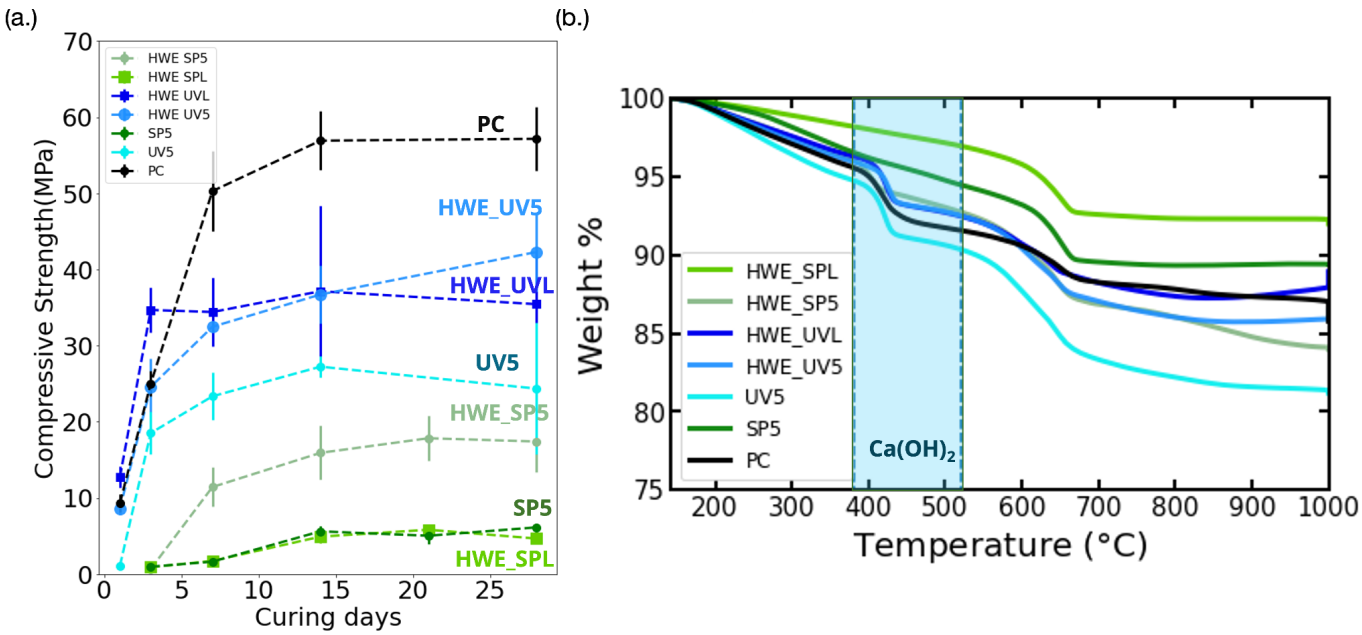

Figure 14. (a.) Compression test result for Hot water extracted spirulina precipitate solid 5%(HWE_SP5) and supernatant liquid (HWE_SPL) cement composite, Hot water extracted ulva precipitate solid 5% (HWE_UV5) supernatant liquid (HWE_UVL) cement composite and compare to PC, UV5, SP5. (b.) TGA results for hot water extracted cement composite compared to PC, UV5, and SP5

The compressive strength of the hot water extracted Spirulina precipitate solid 5% cement composite (HWE_SP5) and hot water extracted Ulva precipitate solid 5% cement composite (HWE_UV5) perform significantly better than their virgin counterparts by 73.6% (42.30 vs. 24.36 MPa). This difference suggests that the extraction procedure performed at 100 °C effectively removes undesirable chemicals that hinder the cement hydration, which water-soluble proteins and polysaccharides may induce. In contrast, the hot water extracted spirulina supernatant liquid cement composite (HWE_SPL) and hot water extracted ulva supernatant liquid cement composite (HWE_UVL) showed lower compressive strength with very low biocomposite percentages (~2 %, back-calculated from mass loss in TGA), which is consistent with the precipitate compression test results. Both supernatant liquid composites show a significant decrease in strength compared to the pure cement samples. Additionally, we find that only SP5 and HWE_SPL do not present a typical $Ca(OH)_2$ decomposition profile in the TGA result (**Figure 14b.)**, implying the main chemical that causes the hindrance of the hydration reaction is extracted from raw spirulina and present in the supernatant through hot water extraction. This finding highlights the importance of characterizing the compositions of the extracted supernatant and the modified algae precipitations in future work.

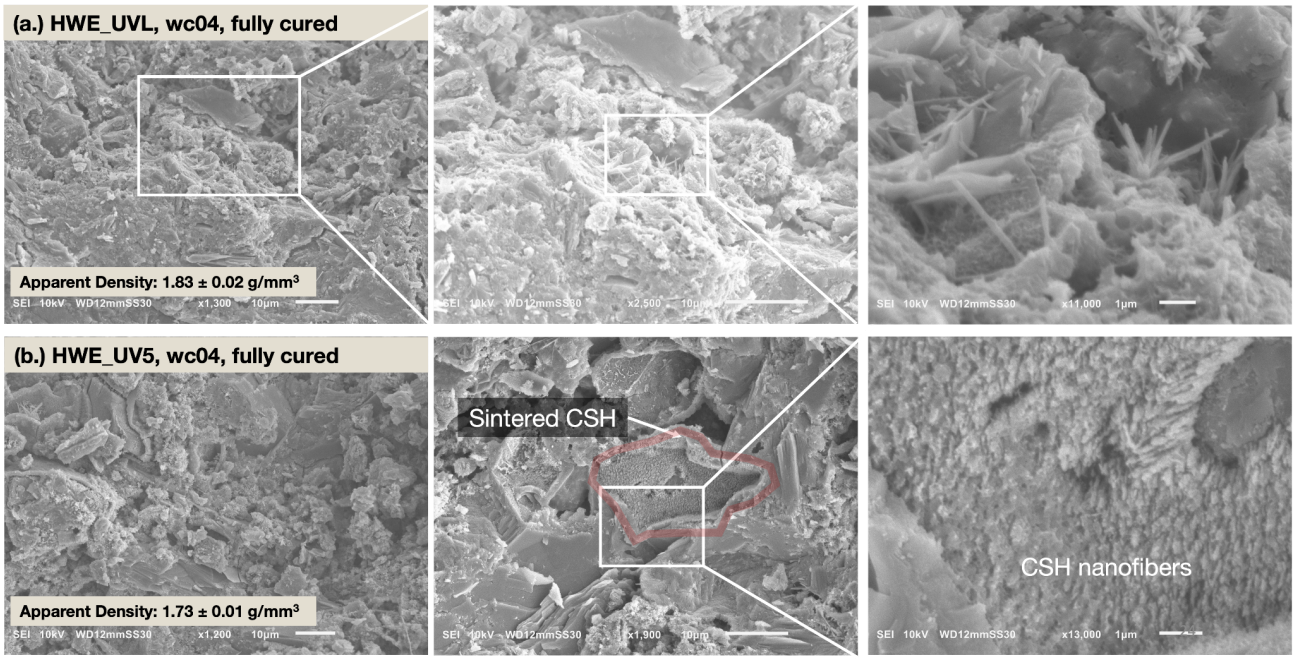

Figure 15. SEM image of the hot water extracted ulva product cement composites. (a.) Hot water extraction ulva supernatant liquid cement composite, w/c = 0.4, fully cured, with an apparent density of 1.83 ± 0.02 g/mm^3 (b.) Hot water extraction ulva precipitate solid cement composite, w/c = 0.4, fully cured, with an apparent density of 1.73 ± 0.01 g/mm^3

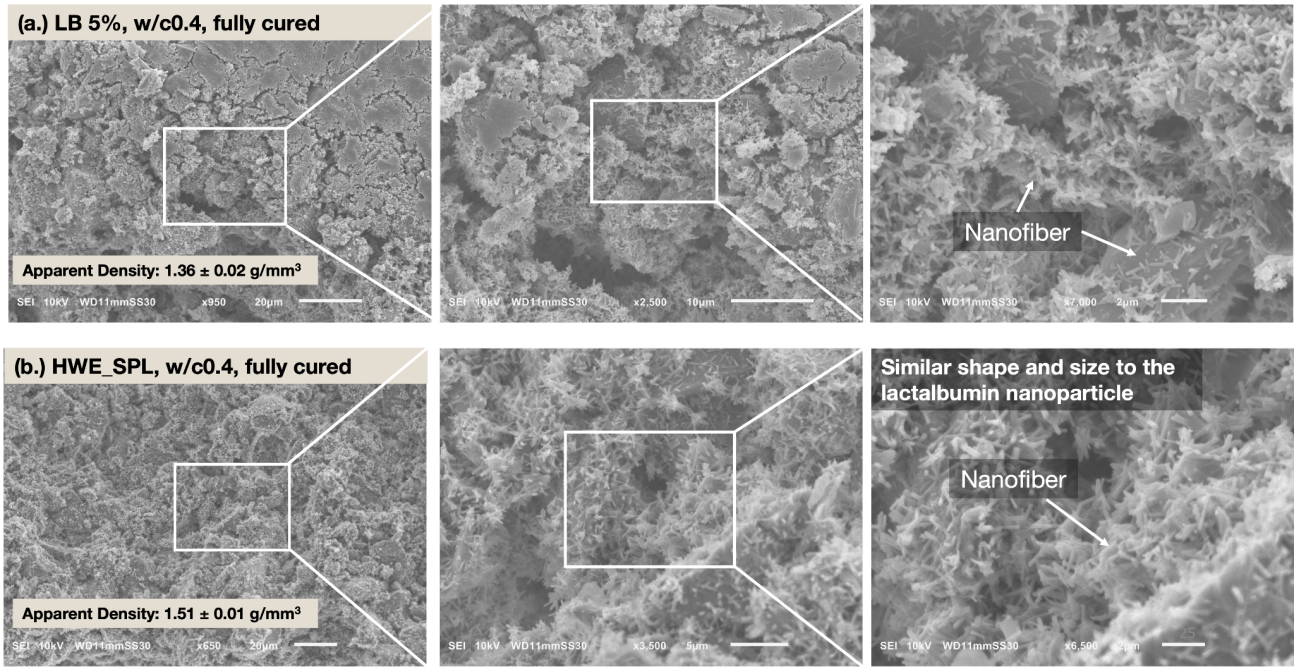

Figure 16. Morphology comparison for HWE_SPL and LB5 (a.) Lactalbumin 5% cement composite, w/c = 0.4, fully cured, with an apparent density of 1.36 ± 0.02 g/mm^3(b.) Hot water extraction spirulina supernatant liquid cement composite, w/c = 0.4, fully cured, with an apparent density of 1.51 ± 0.01g/mm^3

3.3.2 Morphological Analysis

From the SEM image shown in **Figure 15.**, we identify the typical hydration product HWE_UV5 and HWE_UVL in the composite matrix. For example, HWE_UV5 shows sintered CSH product around the supernatant particle and CSH nanofiber within the matrix. In addition, we see the ettringite needles, $Ca(OH)_2$ platelets, and fibrous CSH nanofibers in HWE_UVL at the higher magnification (x11,000). This observation explains the fact that even though the strength of HWE_UVL is lower than pure cement due to the low concentration (~2.1% from the mass loss in TGA) of extracted compounds in the supernatant, the presence of typical hydration products still provides structural compounds for the mechanical properties. Complementarily, the abundant CSH in the modified ulva precipitates composites contributed to the 73.6% improved compressive strength. On the other hand, we observe the distinct nanofibers in the HWE_SPL cement composite (**Figure 16 b.**), similar nanofibers previously identified in the LB5 matrix. This identical microstructure aligns well with our hypothesis that the high protein content in the spirulina biomatter cause the hindrance and the retardation of the hydration reaction and further decrease the final strength of the algae biomatter composite. This also explains the better compression strength of the ulva biomatter cement composites, which have a lower protein percentage across all ulva species than spirulina.

3.3.2 Evaluation Of The Hydration Of Cement Composite

To confirm the presence of hydration products, we investigated representative cement composite samples using FTIR. Analysis of the glucomannan (GM5) and lactalbumin (LB5) samples revealed a lack of peaks at 3643 cm^{-1}, corresponding to the absence of $Ca(OH)_2$. The stearic acid 5% cement composite (SA5) exhibited a unique peak at 2914.5 cm^{-1} and 2849.1 cm^{-1}, attributed to the asymmetric and symmetric stretching vibrations of the $–CH_2–$ band in stearic acid.[8,35,36] We also observed a peak at 1653.5 cm^{-1}, which indicates the presence of H_2O in ettringite, and a peak at 1411.2 cm^{-1}, which indicates the carbonate (CO_3) out-of-plane bending in calcite. Other notable peaks include 1110.6 cm^{-1} for the anti-symmetric SO_4 stretching band in ettringite. Notably, the GM and LB samples showed less distinct and redshifted peaks at 947.8 cm^{-1}, which corresponds to the Si-O in CSH [8,35,36], confirming the nanofibers previously observed in **Figure 15a.**, are distinct from CSH.

Based on the FTIR data presented in **Figure 17.**, it is evident that the glucomannan (GM) and lactalbumin (LB) composites lack the peak of OH in $Ca(OH)_2$ at 3642.7 cm^{-1} and the peak of Si-O in CSH at 950 cm^{-1}. This confirms again with explains the low compressive strength of the composites and the absence of a decomposition profile in the range of 380-520 ℃ in TGA results. The results suggest that both lactalbumin and glucomannan hinder the primary hydration reaction completely, leading to the absence of the $Ca(OH)_2$ peak. However, they still

permit the secondary hydration reaction from tricalcium aluminate, which leads to ettringite production. Notably, the strength of ulva and spirulina composites improved after hot-water extraction, as confirmed by the presence of $Ca(OH)_2$ and CSH, corresponding to the peaks at 3642.7 cm^{-1} and 947.9 cm^{-1}, respectively. This effective pretreatment highlights the need to characterize the water-soluble biopolymers that exist in algal biomatter, especially at high temperature, as they seem responsible for the hindrance effect in the virgin algae-cement composites.

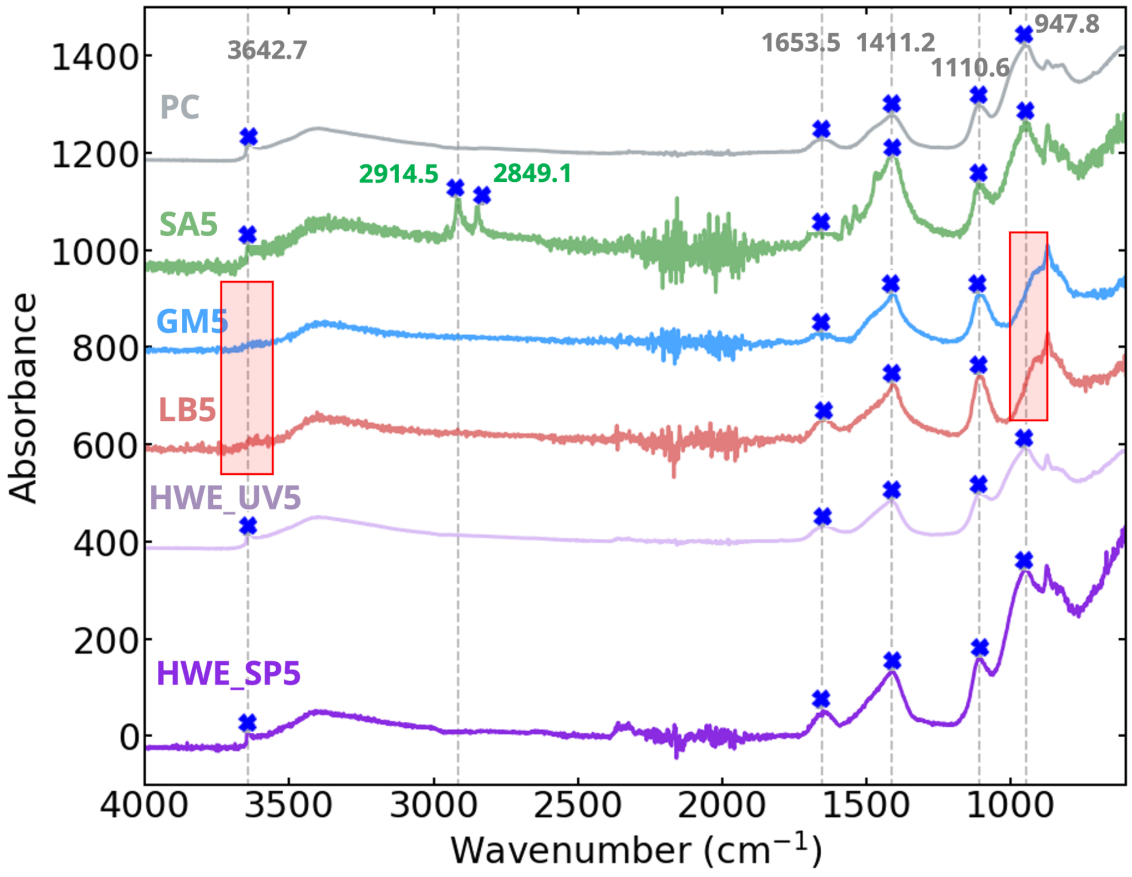

Figure 17. FTIR spectra of biopolymer additive and hot water extraction study cement composite.

3.4 ANALYSIS OF BIOMASS PROTEINS BEHAVIOR IN THE CEMENT MATRIX

Based on the analogous study through representative biopolymers and the pretreated biomatter through extraction methods, we now can conclude that proteins have the most significant chemical interference with the cement hydration reaction, inducing significantly distinct nanofibers within the matrix. It is worth noting that although glucomannan also seriously impacts compressive strength, this may be primarily due to its extreme water uptake ability[33], which prevents the cement from fully hydrating. For further studies of the influence of polysaccharides, we provide insights and future directions in Chapter 5. To further investigate the interrelationship between the biomass proteins and the cement matrix, more specifically on how the proteins perform in cement's extreme environment (high pH and high ionic strength), we conducted a study on lactalbumin under four distinct conditions: alkaline, acid, cement pore water, and calcium chloride solution.

Proteins exhibit primary, secondary, tertiary, and quaternary structures, with the secondary and tertiary structures being more susceptible to environmental effects. This study aims to investigate the impact of the cement matrix on protein structures, focusing on the secondary and tertiary structures. To achieve this, the representative protein chosen in this essay, lactalbumin powder, was subjected to freeze-drying after exposure to four different solution environments for 24hr. We then use FTIR to characterize the bonds of the proteins and the

bonding environment and will provide this as a controlled study to compare with algal proteins in future studies.

The cement environment is known to have a high pH value and high ionic concentration.[38,39] We conducted a pH value test at varying water-to-cement (w/c) ratios to characterize the influence of H^+ and OH^- ions from the slurry on the biopolymer and biomass. This test aimed to establish the relationship between pH and w/c ratios (ranging from 0.4 to 0.6) and determine the alkaline conditions required for subsequent experiments. To determine the pH value of the cement pore water samples, five separate measurements were taken for each sample, and the test was done using a pH Meter (Symphony B10P instrument, VWR). **Figure 18.** illustrates that the w/c ratio in the range of 0.4-0.6 of the cement pore water has a negligible effect on the pH value, with a relatively constant value ranging from 13.0 to 13.3. Consequently, an alkaline solution with a pH of 13, using NaOH, was prepared as a parallel comparison. Additionally, a pH 3 HCl solution was prepared for comparison to investigate the effect of an acidic environment on lactalbumin. Furthermore, existing literature suggests that calcium ions can bind to lactalbumin and stabilize the protein's secondary structure, influencing the denaturation behavior.[40] Considering that the cement pore water contains high levels of calcium ions, a calcium chloride solution was also prepared to investigate the behavior of lactalbumin under a calcium-rich environment.

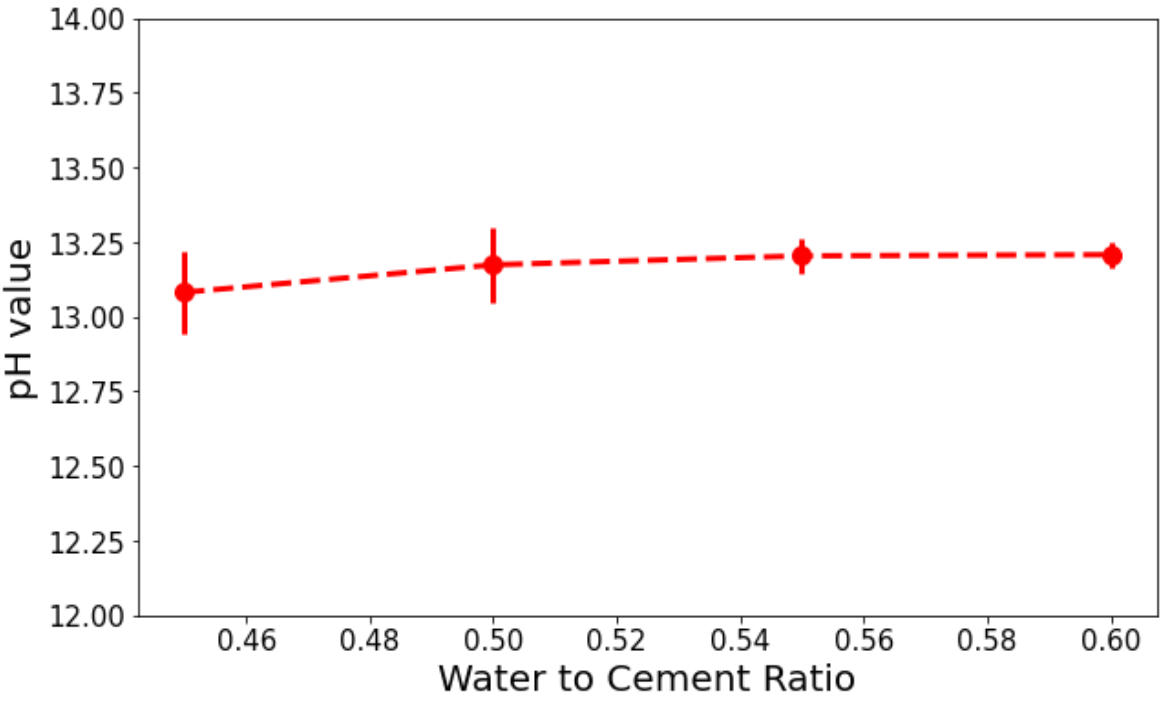

Figure 18. pH value analysis of cement pore water.

In FTIR spectroscopy, the spectra Amide I and Amide II regions are typically examined, as they correspond to the peptide group C=O stretch and in-plane N-H bending/C-N stretching vibrations, respectively. The Amide I band is primarily located within the 1610 cm^{-1} to 1700 cm^{-1} region, while the Amide II band is within 1510 cm^{-1} to 1580 cm^{-1} region. Both regions are sensitive to the secondary structure of proteins.[38-42]

From the FTIR results in **Figure 19.**, we observe a significant peak shift to a higher wavenumber when lactalbumin is subjected to NaOH alkaline conditions, cement porewater (PC suspension), and $CaCl_2$ solution. At the same time, there is a minor peak shift in acid conditions. Based on the literature, the shifting to a higher wavenumber at Amide I peak suggests that under the

NaOH alkaline conditions, cement porewater, and $CaCl_2$ solution conditions, the secondary structure of lactalbumin shifts from a beta-sheet dominant structure to an alpha-helix dominant structure.[40,41] However, further data analysis, such as peak deconvolution, is required to confirm this hypothesis. Nonetheless,calcium-rich and alkaline conditions have shown a greater effect on protein structure in this preliminary test. More characterizations for the effect of environments on the virgin algal biomass are recommended to build up the interrelationships between the algal biomatter and cement matrix.

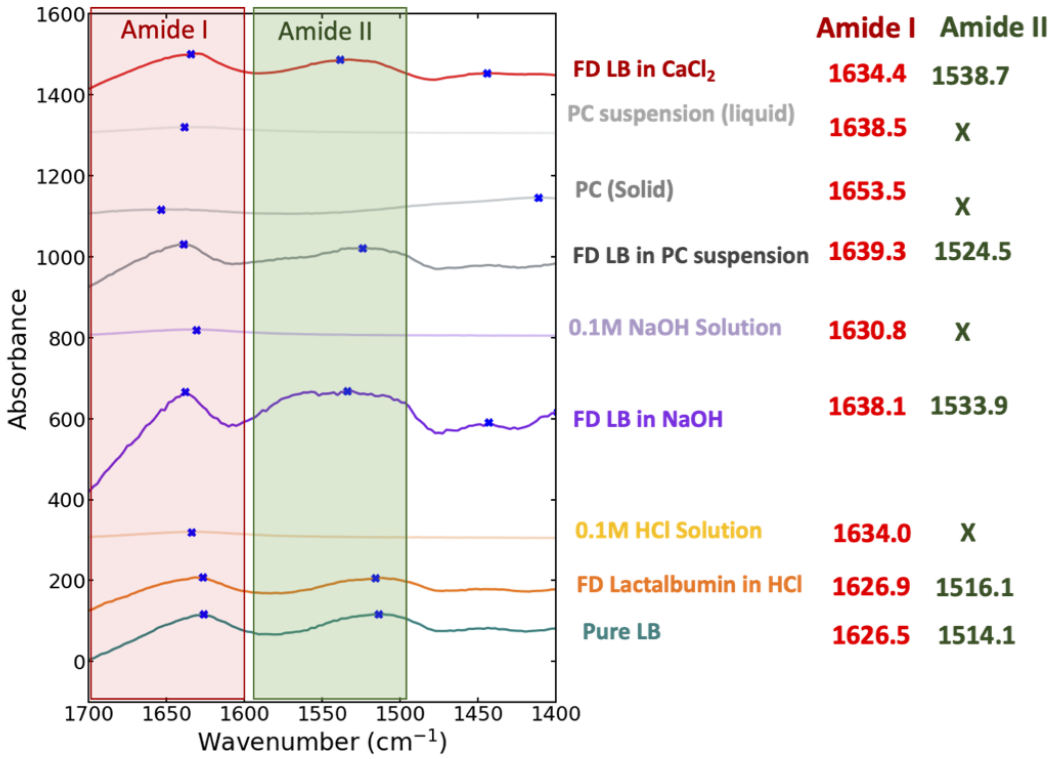

Figure 19. FTIR spectra of lactalbumin

CHAPTER 4 – CONCLUSION

This study aims to provide a comprehensive understanding of the chemical interactions between algae-based biomatter and the cement matrix. Through various characterization methods including mechanical testing, TGA, SEM imaging, FTIR, and EDS analysis, we observed that protein components have a significant influence on hindering and retarding the cement hydration process. Additionally, we observed the formation of distinct nanofibers in 500-700 nm within the lactalbumin cement composite matrix. Furthermore, an investigation of lower percentages of sucrose in the cement composite revealed an unusually low compressive strength at 0.5% sucrose. In comparison, SEM imaging showed a denser matrix in the 5% sucrose cement composite.

To directly examine the impact of removing chemical components that weaken the cement composites, extraction methods were employed on the virgin algal biomatter as a pretreatment. Both hot-water extraction-modified precipitate ulva and spirulina cement composites exhibited improved final compressive strength, suggesting the effective removal of hindering chemicals. This finding is consistent with the results obtained through the supernatant as the control study to compare with pure cement. In addition,

through mechanical testing, SEM imaging, and FTIR analysis of extraction-modified ulva and spirulina cement composites, we observed similar nanofiber morphology in the hot water extraction supernatant spirulina cement composite, akin to the lactalbumin cement composite samples, indicating the correlation between protein and the nanofiber byproduct. These results comply with the finding that hot water extraction pretreatment successfully removes the detrimental water-soluble proteins from virgin spirulina, leading to reduced hindrance and the formation of nanofibers and improved compressive strength. Furthermore, this explains the higher compressive strength observed in the raw Ulva samples.

Finally, the study on biomass proteins revealed a significant effect of pH and calcium cations on inducing secondary structural changes. Both alkaline and high concentration of calcium ion environments exhibited the most pronounced alterations in secondary structure among all the tested conditions. While further investigation is warranted, these findings contribute to our understanding of protein behavior within the cement matrix.

CHAPTER 5 – FUTURE WORK

Although this study has identified proteins as one of the leading chemical components causing hindrance and retardation in algae-based cement composites, there are still several avenues for future research to further validate and expand upon the findings. The following areas of investigation are recommended for future work:

1. Hydration Kinetics: To gain a more comprehensive understanding of the hydration kinetics of both biopolymer representatives and extraction-modified algae cement composites, isothermal calorimetry (IC) and X-ray diffraction (XRD) should be implemented. These techniques will provide valuable insights into the hydration processes and the resulting material properties.

2. Saccharide Retardation Study: Further examination of the effect of sucrose concentration and molecular weight on compressive strength is warranted. Testing a wider range of sucrose concentrations will allow a more thorough observation of the strength evolution. Additionally, employing techniques such as FTIR, IC, and XRD will help elucidate the mechanisms behind the observed retardation phenomenon and clarify whether the sucrose crystals contribute to higher compressive strength at concentrations larger than 3%.

3. Characterization of Extracted Supernatant: Expanding the characterization of the extracted supernatant is recommended. SDS-PAGE analysis can provide insights into the distribution of protein molecular weights, while carbon-hydrogen-nitrogen content analysis (CHN) can further quantify the protein content. Consideration should be given to additional purification steps to simplify the solution system for implementation in cement composites and enable more comprehensive characterization.

4. Evaluation of Hot Water Extracted Supernatant: To further understand the hindrance and retardation effects of hot water-extracted supernatant, it is recommended to quantify the concentrations of the supernatant as an additive. One suggested method is freeze-drying the supernatant and incorporating the solid states extracted additives into cement composites. This will allow for quantitative analysis and directly comparing the same percentage of raw algae and precipitate composite counterparts.

5. Investigation of Cold Water Extraction: Cold water extraction cement composite samples should be further investigated using techniques such as TGA, FTIR, and SEM. This will provide insights into the hydration reactions and the effect of protein denaturation due to the introduction of heat in comparison to the hot water extraction counterpart.

6. Biomass Protein Behavior: Deconvolution of FTIR peaks and further literature review should be undertaken to gain a better understanding of the structure of biomass proteins

within the cement matrix. Combining this with the study of hot and cold water extraction will provide insights into the relationship between the secondary structure of proteins and the evolution of strength in the biomatter cement composite. Furthermore, the study of the impact of the cement environment on the biomass should be extended to the virgin algae based on the peak shift patterns shown by the protein representative in this report.

By addressing these areas of future research, a deeper understanding of the chemical interactions and the behavior of algae-based cement composites can be achieved. This will contribute to developing optimized and sustainable construction materials for future applications.

REFERENCES

[1] U.S. Environmental Protection Agency. (2022, September 19). *Cement Manufacturing Enforcement Initiative.* https://www.epa.gov/enforcement/cement-manufacturing-enforcement-initiative

[2] Singla V. (2022, January 18). Cut Carbon and Toxic Pollution, *Make Cement Clean and Green. Natural Resources Defense Council, Inc.* https://www.nrdc.org/bio/veena-singla/cut-carbon-and-toxic-pollution-make-cement-clean-and-green

[3] Kusuma, R. T., Hiremath, R. B., Rajesh, P., Kumar, B., & Renukappa, S. (2022). Sustainable transition towards biomass-based cement industry: A review. *Renewable and Sustainable Energy Reviews,* 163, 112503.

[4] Rejini Rajamma, Ball RJ, Tarelho LAC, Allen GC, Labrincha JA, Ferreira VM. (2009). Characterization and use of biomass fly ash in cement-based materials. *Journal of Hazardous Materials*, 172(2-3), 1049-1060. ISSN 0304-3894. https://doi.org/10.1016/j.jhazmat.2009.07.109.

[5] Vo, L. T. T., & Navard, P. (2016). Treatments of plant biomass for cementitious building materials – A review. *Construction and Building Materials*, 121, 161-176.

[6] Tonoli, G. H. D., Rodrigues Filho, U. P., Savastano, H., Bras, J., Belgacem, M. N., & Rocco Lahr, F. A. (2009). Cellulose modified fibres in cement based composites. *Composites Part A: Applied Science and Manufacturing, 40*(12), 2046-2053.

[7] Jo, B. W., Chakraborty, S. (2015). A mild alkali treated jute fibre controlling the hydration behaviour of greener cement paste. *Scientific Reports, 5,* 7837. doi: 10.1038/srep07837.

[8] Chen, X., Matar, M. G., Beatty, D. N., & Srubar, W. V. III. (2021). Retardation of Portland Cement Hydration with Photosynthetic Algal Biomass. *ACS Sustainable Chemistry & Engineering, 9*(41), 13726-13734. https://doi.org/10.1021/acssuschemeng.1c04033

[9] Hernandeza, E., Cano-Barritaa, P.F., & Torres-Acostab, A.A. (2015). Influence of cactus mucilage and marine brown algae extract on the compressive strength and durability of concrete.

[10] León-Martínez, F. M., Cano-Barrita, P. F. de J., Lagunez-Rivera, L., & Medina-Torres, L. (2014). Study of nopal mucilage and marine brown algae extract as viscosity-enhancing admixtures for cement based materials. *Construction and Building Materials,* 53, 190-202.

[11] Chahbi, M., Mortadi, A., El Moznine, R., Monkade, M., Zaim, S., Nmila, R., & Rchid, H. (2022). A new approach to investigate the hydration process and the effect of algae powder on the strength properties of cement paste. *Australian Journal of Mechanical Engineering.* Advance online publication. https://doi.org/10.1080/14484846.2022.2066855

[12] Murugappan, V., & Muthadhi, A. (2022). Studies on the influence of alginate as a natural polymer in mechanical and long-lasting properties of concrete - A review. *Materials Today: Proceedings, 65*(Part 2), 839-845. ISSN 2214-7853. https://doi.org/10.1016/j.matpr.2022.03.424.

[13] Karthick Srinivas M, Alengaram UJ, Ibrahim S, Phang SM, Vello V, Jun HK, Alnahhal AM. (2021). Evaluation of crack healing potential of cement mortar incorporated with blue-green microalgae. *Journal of Building Engineering*, 44, 102958. ISSN 2352-7102. https://doi.org/10.1016/j.jobe.2021.102958.

[14] Mamlouk, M., & Zaniewski, J. (1999). Materials for Civil and Construction Engineers. Addison Wesley Longman.

[15] Double, D. D., Hewlett, P. C., Sing, K. S. W., & Raffle, J. F. (1983). New Developments in Understanding the Chemistry of Cement Hydration [and Discussion]. *Philosophical Transactions of the Royal Society of London. Series A, Mathematical and Physical Sciences, 310*(1511), 53–66. http://www.jstor.org/stable/37463

[16] Mehta, P.K. (1976). Scanning electron micrographic studies of ettringite formation. *Cement and Concrete Research, 6*, 169-182.

[17] Luo, S., Liu, M., Yang, L., & Chang, J. (2019). Effects of drying techniques on the crystal structure and morphology of ettringite. Construction and Building Materials.

[18]Ciferri, O., & Tiboni, O. (1985). The biochemistry and industrial potential of Spirulina. *Ann. Rev. Microbiol., 39*, 503-526.

[19]Markou, G., Chatzipavlidis, I., & Georgakakis, D. (2012). Carbohydrates production and bio-flocculation characteristics in cultures of Arthrospira (Spirulina) platensis: Improvements through phosphorus limitation process. *Bioenergy Research*, 5, 915-925. https://doi.org/10.1007/s12155-012-9205-3

[20]Largo, D. B., Sembrano, J., Hiraoka, M., & et al. (2004). Taxonomic and ecological profile of 'green tide' species of Ulva (Ulvales, Chlorophyta) in central Philippines. *Hydrobiologia, 512*, 247-253. https://doi.org/10.1023/B:HYDR.0000020333.33039.4b

[21] Yaich, H., Garna, H., Besbes, S., Paquot, M., Blecker, C., & Attia, H. (2011). Chemical composition and functional properties of Ulva lactuca seaweed collected in Tunisia. *Food Chemistry, 128*(4), 895-901. https://doi.org/10.1016/j.foodchem.2011.03.114

[22] Osuna-Ruiz, I., Nieves-Soto, M., Manzano-Sarabia, M., Garibay, E., Lizardi-Mendoza, J., Burgos-Hernández, A., & Hurtado-Oliva, M. (2019). Gross chemical composition, fatty acids, sterols, and pigments in tropical seaweed species off Sinaloa, Mexico. *Ciencias Marinas, 45*(3), 101-120. https://doi.org/10.7773/cm.v45i3.2974

[23] Osuna-Ruiz, I., Nieves-Soto, M., Manzano-SaraFlores-Chaparro, C. E., Chazaro Ruiz, L. F., Alfaro de la Torre, M. C., Huerta-Diaz, M. A., Rangel-Mendez, J. R. (2017). Biosorption removal of benzene and toluene by three dried macroalgae at different ionic strength and temperatures: Algae biochemical composition and kinetics. *Journal of Environmental Management, 193*, 126-135. https://doi.org/10.1016/j.jenvman.2017.02.005

[24] Peña-Rodríguez, A., Mawhinney, T. P., Ricque-Marie, D., & Cruz-Suárez, L. E. (2011). Chemical composition of cultivated seaweed Ulva clathrata (Roth) C. Agardh. *Food chemistry, 129*(2), 491–498. https://doi.org/10.1016/j.foodchem.2011.04.104

[25] Bensehaila, S., Doumandji, A., Boutekrabt, L., Manafikhi, H., Peluso, I., Bensehaila, K., Kouache, A., & Bensehaila, A. (2015). The nutritional quality of Spirulina platensis of Tamenrasset, Algeria. *African Journal of Biotechnology,* 14, 1649-1654. DOI: 10.5897/AJB2015.14414.

[26] Oliveira, M. d., Monteiro, M., Robbs, P., Pereira, S., & Moraes, L. P. G. (1999). Growth and chemical composition of Spirulina maxima and Spirulina platensis biomass at different temperatures. *Aquaculture International, 7*, 261-275. https://doi.org/10.1023/A:1009233230706

[27] Shekharam, K. Madhavi, Raghuramulu Naidu, Satyanarayana Rao, and Rao Vadaparthi. "Carbohydrate composition and characterization of two unusual sugars from the blue green alga, Spirulina platensis." *Phytochemistry 26* (1987): 2267-2269.

[28] Kusmiyati, Kusmiyati, Retno Wulan Sari, Muchalal Muchalal, and Herry Suhardiyanto. "Hydrolysis of Microalgae Spirulina platensis, Chlorella sp., and Macroalgae Ulva lactuca for Bioethanol Production." *International Energy Journal 20* (2020): 611-620.

[29] Chaiklahan, R., Chirasuwan, N., Triratana, P., Loha, V., Tia, S., & Bunnag, B. (2013). Polysaccharide extraction from Spirulina sp. and its antioxidant capacity. *International journal of biological macromolecules, 58*, 73–78. https://doi.org/10.1016/j.ijbiomac.2013.03.046

[30] Chi, Y., Li, Y., Zhang, G., Gao, Y., Ye, H., Gao, J., & Wang, P. (2018). Effect of extraction techniques on properties of polysaccharides from Enteromorpha prolifera and their applicability

in iron chelation. *Carbohydrate polymers, 181*, 616–623. https://doi.org/10.1016/j.carbpol.2017.11.104

[31] Wassie, T., Niu, K., Xie, C., Wang, H., & Xin, W. (2021). Extraction Techniques, Biological Activities and Health Benefits of Marine Algae Enteromorpha prolifera Polysaccharide. *Frontiers in nutrition, 8*, 747928. https://doi.org/10.3389/fnut.2021.747928

[32] Manrich, A., Oliveira, J., Martins, M., & Mattoso, L. (2020). Physicochemical and Thermal Characterization of the Spirulina platensis. *Journal of Agricultural Science and Technology B*, 10. https://doi.org/10.17265/2161-6264/2020.05.004.

[33] Keithley, J. K., Swanson, B., Mikolaitis, S. L., DeMeo, M., Zeller, J. M., Fogg, L., Adamji, J. (2013). Safety and Efficacy of Glucomannan for Weight Loss in Overweight and Moderately Obese Adults. *Journal of Obesity*, vol. 2013, Article ID 610908, 7 pages. https://doi.org/10.1155/2013/610908

[34] Singh, L. P., Goel, A., Bhattachharyya, S., Ahalawat, S., Sharma, U., & Mishra, G. (2015). Effect of morphology and dispersibility of silica nanoparticles on the mechanical behaviour of cement mortar. *International Journal of Concrete Structures and Materials, 9*. https://doi.org/10.1007/s40069-015-0099-2

[35] Lin, M.-Y., Grandgeorge, P., Jimenez, A. M., Nguyen, B. H., & Roumeli, E. (2022). Long-Term Hindrance Effects of Algal Biomatter on the Hydration Reactions of Ordinary Portland Cement.

ACS Sustainable Chemistry & Engineering, Article ASAP.
https://doi.org/10.1021/acssuschemeng.2c07539

[36]Thiery, V., Dubois, E., & Bellayer, S. (2022). The good, the bad and the ugly polishing: Effect of abrasive size on standardless EDS analysis of Portland cement clinker's calcium silicates. *Micron (Oxford, England : 1993)*, 158, 103266. https://doi.org/10.1016/j.micron.2022.103266

[37] Yang, H., Monasterio, M., Cui, H., & Han, N. (2017). Experimental study of the effects of graphene oxide on microstructure and properties of cement paste composite. *Composites Part A: Applied Science and Manufacturing*, 102, 263-272.
https://doi.org/10.1016/j.compositesa.2017.07.022

[38] Byfors, K. (1987). Influence of silica fume and flyash on chloride diffusion and pH values in cement paste. *Cement and Concrete Research, 17*(1), 115-130.
https://doi.org/10.1016/0008-8846(87)90066-4

[39] Sumra, Y., Payam, S., & Zainah, I. (2020). The pH of cement-based materials: A review. *Journal of Wuhan University of Technology-Materials Science Edition, 35*, 908-924.
https://doi.org/10.1007/s11595-020-2337-y

[38] Grdadolnik, J. (2003). Saturation effects in FTIR spectroscopy: intensity of amide I and amide II bands in protein spectra. *Acta chimica slovenica,* 50(4), 777-788.

[39] Wi, S., Pancoska, P., & Keiderling, T. A. (1998). Predictions of protein secondary structures using factor analysis on Fourier transform infrared spectra: Effect of Fourier self-deconvolution of the amide I and amide II bands. *Biospectroscopy*, 4(2), 93-106.

[40] Mizuguchi, M., Nara, M., Kawano, K., & Nitta, K. (1997). FT-IR study of the Ca^{2+}-binding to bovine alpha-lactalbumin. Relationships between the type of coordination and characteristics of the bands due to the Asp COO^- groups in the Ca^{2+}-binding site. *FEBS letters*, 417(1), 153–156. https://doi.org/10.1016/s0014-5793(97)01274-x

[41] Boye, J. I., Alli, I., & Ismail, A. A. (1997). Use of Differential Scanning Calorimetry and Infrared Spectroscopy in the Study of Thermal and Structural Stability of α-Lactalbumin. *Journal of Agricultural and Food Chemistry, 45*(4), 1116-1125. https://doi.org/10.1021/jf960360z

[42] Zhong, H., Gilmanshin, R., & Callender, R. (1999). An FTIR Study of the Complex Melting Behavior of α-Lactalbumin. *Journal of Physical Chemistry B, 103*(19), 3947-3953.